PHYSICAL REVIEW D **95,** 115008 (2017)

# Combined analysis of semileptonic $B$ decays to $D$ and $D^*$: $R(D^{(*)})$, $|V_{cb}|$, and new physics

Florian U. Bernlochner,[1] Zoltan Ligeti,[2] Michele Papucci,[2] and Dean J. Robinson[3]

[1]*Physikalisches Institut der Rheinischen Friedrich-Wilhelms-Universität Bonn, 53115 Bonn, Germany*
[2]*Ernest Orlando Lawrence Berkeley National Laboratory, University of California, Berkeley, California 94720, USA*
[3]*Physics Department, University of Cincinnati, Cincinnati, Ohio 45221, USA*

(Received 4 April 2017; published 8 June 2017)

The measured $\bar{B} \to D^{(*)} l\bar{\nu}$ decay rates for light leptons ($l = e, \mu$) constrain all $\bar{B} \to D^{(*)}$ semileptonic form factors, by including both the leading and $\mathcal{O}(\Lambda_{\rm QCD}/m_{c,b})$ subleading Isgur-Wise functions in the heavy quark effective theory. We perform a novel combined fit to the $\bar{B} \to D^{(*)} l\bar{\nu}$ decay distributions to predict the $\bar{B} \to D^{(*)}\tau\bar{\nu}$ rates and determine the Cabibbo-Kobayashi-Maskawa matrix element $|V_{cb}|$. Most theoretical and experimental papers have neglected uncertainties in the predictions for form factor ratios at order $\Lambda_{\rm QCD}/m_{c,b}$, which we include. We also calculate $\mathcal{O}(\Lambda_{\rm QCD}/m_{c,b})$ and $\mathcal{O}(\alpha_s)$ contributions to semileptonic $\bar{B} \to D^{(*)}\ell\bar{\nu}$ decays for all possible $b \to c$ currents. This result has not been available for the tensor current form factors, and for two of those, which are $\mathcal{O}(\Lambda_{\rm QCD}/m_{c,b})$, the corrections are of the same order as approximations used in the literature. These results allow us to determine with improved precision how new physics may affect the $\bar{B} \to D^{(*)}\tau\bar{\nu}$ rates. Our predictions can be systematically improved with more data; they need not rely on lattice QCD results, although these can be incorporated.

DOI: 10.1103/PhysRevD.95.115008

## I. INTRODUCTION

Heavy quark symmetry [1,2] plays an essential role in understanding exclusive semileptonic $b \to c\ell\bar{\nu}$ mediated transitions, by providing relations between hadronic form factors. At leading order in $\Lambda_{\rm QCD}/m_{c,b}$, the symmetry also determines the absolute normalization of form factors at the "zero recoil" point, $v_B = v_{D^{(*)}}$, corresponding to maximal invariant mass, $q^2$, of the outgoing lepton pair. Incorporating small corrections to the symmetry limit permits a (hadronic) model-independent determination of $|V_{cb}|$ from exclusive decays. Recently, the *BABAR* [3,4], Belle [5–7], and LHCb [8] measurements of the $|V_{cb}|$-independent ratios

$$R(D^{(*)}) = \frac{\Gamma(\overline{B} \to D^{(*)}\tau\bar{\nu})}{\Gamma(\overline{B} \to D^{(*)} l\bar{\nu})}, \qquad l = \mu, e, \tag{1}$$

renewed interest in these decays. The world average of $R(D)$ and $R(D^*)$ is in tension with the standard model (SM) expectation at the $4\sigma$ level [9]. This is intriguing as it occurs in a tree-level SM process, while most new physics (NP) explanations require new states at or below one TeV [10].

Besides the search for new physics, understanding $b \to c\ell\bar{\nu}$ mediated semileptonic decays as precisely as possible is also important for future improvements of the determinations of the Cabibbo-Kobayashi-Maskawa elements $|V_{cb}|$ and $|V_{ub}|$, both from exclusive and inclusive $B$ decays, which exhibit some tensions [9]. Depending on the particular measurement, some decay modes contribute to the signals, some to the backgrounds. Future progress is essential for increasing the scale of new physics probed by the Belle II and LHCb experiments [11].

The main uncertainty in predicting $R(D^{(*)})$ comes from the fact that the $\overline{B} \to D^{(*)}\tau\bar{\nu}$ decay rates depend on certain form factors, that only give $m_l^2/m_B^2$ suppressed contributions to the differential rates for the precisely measured light lepton channels. Using heavy quark effective theory (HQET), however, all $\overline{B} \to D^{(*)}$ form factors are described by a single Isgur-Wise function in the $m_{c,b} \gg \Lambda_{\rm QCD}$ limit. At order $\Lambda_{\rm QCD}/m_{c,b}$, only three additional functions of $q^2$ are needed to parametrize all form factors.

We perform the first combined fit to $\overline{B} \to D^{(*)} l\bar{\nu}$ differential rates and angular distributions, including $\mathcal{O}(\Lambda_{\rm QCD}/m_{c,b}, \alpha_s)$ terms in HQET, to constrain both the leading and three subleading Isgur-Wise functions. This fit constrains all form factors, up to higher-order corrections, with uncertainties suppressed by $\mathcal{O}(\Lambda_{\rm QCD}^2/m_{c,b}^2, \alpha_s\Lambda_{\rm QCD}/m_{c,b}, \alpha_s^2)$. We extract $|V_{cb}|$ and form factor ratios under various fit scenarios, that include or omit lattice QCD and/or QCD sum rule inputs, and which provide checks of previously untested theory assumptions or results. Most prior theoretical and experimental studies neglected HQET relations for the form factors at order $\Lambda_{\rm QCD}/m_{c,b}$ or the correlations of the uncertainties in the deviations from the heavy quark limit. Our fits fully incorporate these. These fits also allow precise predictions of the $\overline{B} \to D^{(*)}\tau\bar{\nu}$ rates and $R(D^{(*)})$. Our predictions can be systematically improved with more $\overline{B} \to D^{(*)} l\bar{\nu}$ data, and need not rely on lattice QCD results. A similar approach to

 

analyze $\overline{B} \to D^{**} l \bar{\nu}$ decays was recently carried out in Ref. [12].

We also compute, for all possible $b \to c$ currents, the $\mathcal{O}(\Lambda_{\rm QCD}/m_{c,b})$ and $\mathcal{O}(\alpha_s)$ contributions to the form factors. While the $\mathcal{O}(\Lambda_{\rm QCD}/m_{c,b})$ corrections to the vector and axial-vector matrix elements have been known for over 25 years [13,14], the corrections for the tensor current form factors are not explicitly available in past literature. Two of these form factors vanish in the heavy quark limit, and receive unsuppressed corrections to the partial results, also of order $\Lambda_{\rm QCD}/m_{c,b}$, used previously in the literature.

Section II contains the HQET calculations of the form factors, including order $\Lambda_{\rm QCD}/m_{c,b}$ and $\alpha_s$ contributions, corresponding expressions for form factor ratios, and some details of our numerical evaluations in the $1S$ scheme to avoid known bad behaviors in the perturbation expansions. In Sec. III we review analyticity constraints on the form factors, parametrizations of the Isgur-Wise functions, and develop several fit scenarios consistent with HQET, which we apply to the data. The results for $|V_{cb}|$, form factor ratios, and $R(D^{(*)})$ are discussed. Section IV concludes.

## II. ELEMENTS OF HQET

### A. Matrix elements to order $\Lambda_{\rm QCD}/m_{c,b}$ and $\alpha_s$

We are concerned with matrix elements $\langle D^{(*)}|O_\Gamma|\overline{B}\rangle$, where a full operator basis is

$$\begin{aligned} &O_S = \bar{c} b, \qquad O_P = \bar{c}\gamma^5 b, \qquad O_V = \bar{c}\gamma^\mu b, \\ &O_A = \bar{c}\gamma^\mu\gamma^5 b, \qquad O_T = \bar{c}\sigma^{\mu\nu} b, \end{aligned} \tag{2}$$

with $\sigma^{\mu\nu} \equiv (i/2)[\gamma^\mu, \gamma^\nu]$. [The sign convention is fixed by $\sigma^{\mu\nu}\gamma^5 \equiv -(i/2)\epsilon^{\mu\nu\rho\sigma}\sigma_{\rho\sigma}$, which implies $\mathrm{Tr}[\gamma^\mu\gamma^\nu\gamma^\sigma\gamma^\rho\gamma^5] = +4i\epsilon^{\mu\nu\rho\sigma}$.] The construction of the HQET expansion to order $\mathcal{O}(\Lambda_{\rm QCD}/m_{c,b})$ and $\mathcal{O}(\alpha_s)$ was developed in the early 1990s [15,16]; we summarize here the central elements to establish our conventions.

The HQET allows model-independent parametrization of the spectroscopy of heavy mesons and some hadronic matrix elements between them. The ground-state heavy quark spin symmetry doublet pseudoscalar ($P$) and vector ($V$) mesons correspond to the light degrees of freedom (the "brown muck") in a spin-$\frac{1}{2}$ state combined with the heavy quark spin. They form two states with angular momentum $J_{V,P} = \frac{1}{2} \pm \frac{1}{2}$. Their masses can be expressed as

$$m_{V,P} = m_Q + \bar{\Lambda} - \frac{\lambda_1}{2m_Q} \pm \frac{(2J_{P,V}+1)\lambda_2}{2m_Q} + \cdots, \tag{3}$$

where $m_Q$ is the heavy quark mass parameter of HQET, $\bar{\Lambda} = \mathcal{O}(\Lambda_{\rm QCD})$, $\lambda_{1,2} = \mathcal{O}(\Lambda_{\rm QCD}^2)$, etc. To evaluate matrix elements relevant for semileptonic decays, it is simplest to use the trace formalism [17–19]. Including $\Lambda_{\rm QCD}/m_{c,b}$ corrections, the $B \to D^{(*)}$ matrix elements can be written as [20]

$$\begin{aligned} \frac{\langle D^{(*)}|\bar{c}\Gamma b|\overline{B}\rangle}{\sqrt{m_{D^{(*)}} m_B}} = -\xi(w)\{&\mathrm{Tr}[\bar{H}^{(c)}_{v'}\Gamma H^{(b)}_v] + \varepsilon_c \mathrm{Tr}[\bar{H}^{(c,1)}_{v',v}\Gamma H^{(b)}_v] \\ &+ \varepsilon_b \mathrm{Tr}[\bar{H}^{(c)}_{v'}\Gamma H^{(b,1)}_{v,v'}]\}, \end{aligned} \tag{4}$$

where $\varepsilon_{c,b} = \bar{\Lambda}/(2m_{c,b})$ and $\Gamma$ is an arbitrary Dirac matrix. The pseudoscalar and vector mesons can be represented by a "superfield," which has the right transformation properties under heavy quark and Lorentz symmetry,

$$H^{(Q)}_v = \frac{1+\not{v}}{2}(V^{(Q)}_v \not{\epsilon} - P^{(Q)}_v \gamma_5). \tag{5}$$

The $\Lambda_{\rm QCD}/m_{c,b}$ corrections can be parametrized via [20]

$$\begin{aligned} H^{(Q,1)}_{v,v'} = &\frac{1+\not{v}}{2}\{V^{(Q)}_v[\not{\epsilon}\hat{L}_2(w) + \epsilon\cdot v'\hat{L}_3(w)] - P^{(Q)}_v\gamma_5\hat{L}_1(w)\} \\ &+ \frac{1-\not{v}}{2}\{V^{(Q)}_v[\not{\epsilon}\hat{L}_5(w) + \epsilon\cdot v'\hat{L}_6(w)] - P^{(Q)}_v\gamma_5\hat{L}_4(w)\}. \end{aligned} \tag{6}$$

It is convenient to use the dimensionless kinematic variable $w$ instead of $q^2 = (p_B - p_{D^{(*)}})^2$,

$$w = v\cdot v' = \frac{m_B^2 + m_{D^{(*)}}^2 - q^2}{2m_B m_{D^{(*)}}}, \quad v = \frac{p_B}{m_B}, \quad v' = \frac{p_{D^{(*)}}}{m_{D^{(*)}}}. \tag{7}$$

In Eq. (4) and hereafter, we absorb into the leading-order Isgur-Wise function a heavy quark spin symmetry conserving $\mathcal{O}(\Lambda_{\rm QCD}/m_{c,b})$ subleading term, which does not affect any model-independent predictions of HQET, via $\xi(w) \to \xi(w) + 2(\varepsilon_c + \varepsilon_b)\chi_1(w)$. The function $\chi_1$ parametrizes the matrix element of the time-ordered product of the kinetic operator in the subleading HQET Lagrangian, $O_{\rm kin} = \bar{h}_v(iD)^2 h_v/(2m_Q)$, with the leading-order current. It satisfies $\chi_1(1) = 0$ [13], and hence $\xi(1) = 1$ is maintained. Reparametrization invariance [21] ensures that this redefinition of $\xi(w)$ is scale independent.

The $w$-dependent $L_{1\ldots6}$ functions are [20]

$$\begin{aligned} &\hat{L}_1 = -4(w-1)\hat{\chi}_2 + 12\hat{\chi}_3, \qquad \hat{L}_2 = -4\hat{\chi}_3, \qquad \hat{L}_3 = 4\hat{\chi}_2, \\ &\hat{L}_4 = 2\eta - 1, \qquad \hat{L}_5 = -1, \qquad \hat{L}_6 = -2(1+\eta)/(w+1). \end{aligned} \tag{8}$$

Here the $\hat{\chi}_{2,3}$ terms in $\hat{L}_{1,2,3}$ originate from the matrix elements of the time-ordered product of the leading-order current with the chromomagnetic correction to the Lagrangian, $O_{\rm mag} = (g_s/2)\bar{h}_v\sigma_{\mu\nu}G^{\mu\nu}h_v/(2m_Q)$. Luke's theorem implies $\hat{\chi}_3(1) = 0$ [13]. The $\hat{L}_{4,5,6}$ terms arise from $\Lambda_{\rm QCD}/m_{c,b}$ corrections in the matching of the

$\bar{c}\Gamma b$ heavy quark current onto HQET, $\bar{c}\Gamma b \to \overline{c}_{v'}[\Gamma - i\not{D}\Gamma/(2m_c) + \Gamma i\not{D}/(2m_b) + \cdots]b_v$.[1]

The perturbative corrections to the heavy quark currents may be computed by matching QCD onto HQET [17,26,27]. At $\mathcal{O}(\alpha_s)$, the following operators are generated:

$$\begin{aligned}
\bar{c}b &\to \bar{c}_{v'}(1+\hat{\alpha}_s C_S)b_v,\\
\bar{c}\gamma^5 b &\to \bar{c}_{v'}(1+\hat{\alpha}_s C_P)\gamma^5 b_v,\\
\bar{c}\gamma^\mu b &\to \bar{c}_{v'}[(1+\hat{\alpha}_s C_{V_1})\gamma^\mu + \hat{\alpha}_s C_{V_2} v^\mu + \hat{\alpha}_s C_{V_3} v'^\mu]b_v,\\
\bar{c}\gamma^\mu\gamma^5 b &\to \bar{c}_{v'}[(1+\hat{\alpha}_s C_{A_1})\gamma^\mu + \hat{\alpha}_s C_{A_2} v^\mu + \hat{\alpha}_s C_{A_3} v'^\mu]\gamma^5 b_v\\
\bar{c}\sigma^{\mu\nu} b &\to \bar{c}_{v'}[(1+\hat{\alpha}_s C_{T_1})\sigma^{\mu\nu} + \hat{\alpha}_s C_{T_2} i(v^\mu\gamma^\nu - v^\nu\gamma^\mu)\\
&\quad + \hat{\alpha}_s C_{T_3} i(v'^\mu\gamma^\nu - v'^\nu\gamma^\mu)\\
&\quad + C_{T_4}(v'^\mu v^\nu - v'^\nu v^\mu)]b_v,
\end{aligned} \tag{9}$$

where the $C_{\Gamma_i}$ are functions of $w$ and $z = m_c/m_b$, and $\hat{\alpha}_s = \alpha_s/\pi$. (We follow the notation of Ref. [15], while Ref. [16] used $C_i = \hat{\alpha}_s C_{V_i} + \delta_{i1}$ and $C_i^5 = \hat{\alpha}_s C_{A_i} + \delta_{i1}$.) Evaluating these contributions using the leading-order trace in Eq. (4) leads to $\mathcal{O}(\alpha_s)$ modifications of the coefficients of the Isgur-Wise function, $\xi(w)$. In this paper we neglect $\mathcal{O}(\alpha_s\varepsilon_{c,b})$ corrections, which can also be included straightforwardly (and should be, if NP is established).

The $\alpha_s$ corrections for all five currents were computed in Ref. [27]. Appendix A contains their explicit expressions, at arbitrary matching scale $\mu$. The vector and axial-vector currents are not renormalized in QCD, but the corresponding heavy quark currents have nonzero anomalous dimensions, leading to $\mu$ dependence for $C_{V_1}$ and $C_{A_1}$ for $w \neq 1$. The scalar, pseudoscalar, and tensor currents are renormalized in QCD, and thus $C_S$, $C_P$, and $C_{T_1}$ are also $\mu$ dependent. In the $\overline{\rm MS}$ scheme with dimensional regularization, the remaining $C_{\Gamma_j}$ ($j \geq 2$) are scale independent.

### B. $\overline{B} \to D^{(*)}$ form factors

We use the standard definitions of the form factors. For $\overline{B} \to D$ decays,

$$\langle D|\bar{c}b|\overline{B}\rangle = \sqrt{m_B m_D}\, h_S(w+1), \tag{10a}$$

$$\langle D|\bar{c}\gamma^5 b|\overline{B}\rangle = \langle D|\bar{c}\gamma^\mu\gamma^5 b|\overline{B}\rangle = 0, \tag{10b}$$

$$\langle D|\bar{c}\gamma^\mu b|\overline{B}\rangle = \sqrt{m_B m_D}[h_+(v+v')^\mu + h_-(v-v')^\mu], \tag{10c}$$

$$\langle D|\bar{c}\sigma^{\mu\nu} b|\overline{B}\rangle = i\sqrt{m_B m_D}[h_T(v'^\mu v^\nu - v'^\nu v^\mu)], \tag{10d}$$

while for the $\overline{B} \to D^*$ transitions,

$$\langle D^*|\bar{c}b|\overline{B}\rangle = 0, \tag{11a}$$

$$\langle D^*|\bar{c}\gamma^5 b|\overline{B}\rangle = -\sqrt{m_B m_{D^*}}\, h_P(\epsilon^*\cdot v), \tag{11b}$$

$$\langle D^*|\bar{c}\gamma^\mu b|\overline{B}\rangle = i\sqrt{m_B m_{D^*}}\, h_V \varepsilon^{\mu\nu\alpha\beta}\epsilon^*_\nu v'_\alpha v_\beta, \tag{11c}$$

$$\begin{aligned}
\langle D^*|\bar{c}\gamma^\mu\gamma^5 b|\overline{B}\rangle = \sqrt{m_B m_{D^*}}[&h_{A_1}(w+1)\epsilon^{*\mu}\\
&- h_{A_2}(\epsilon^*\cdot v)v^\mu - h_{A_3}(\epsilon^*\cdot v)v'^\mu],
\end{aligned} \tag{11d}$$

$$\begin{aligned}
\langle D^*|\bar{c}\sigma^{\mu\nu} b|\overline{B}\rangle = -\sqrt{m_B m_{D^*}}\varepsilon^{\mu\nu\alpha\beta}[&h_{T_1}\epsilon^*_\alpha(v+v')_\beta\\
&+ h_{T_2}\epsilon^*_\alpha(v-v')_\beta\\
&+ h_{T_3}(\epsilon^*\cdot v)v_\alpha v'_\beta].
\end{aligned} \tag{11e}$$

The $i$, $-1$, and $w+1$ factors are chosen such that in the heavy quark limit each form factor either vanishes or equals the leading-order Isgur-Wise function,

$$\begin{aligned}
&h_- = h_{A_2} = h_{T_2} = h_{T_3} = 0,\\
&h_+ = h_V = h_{A_1} = h_{A_3} = h_S = h_P = h_T = h_{T_1} = \xi.
\end{aligned} \tag{12}$$

Using Eqs. (4) and (9), one can compute all form factors to order $\mathcal{O}(\Lambda_{\rm QCD}/m_{c,b})$ and $\mathcal{O}(\alpha_s)$. It is convenient to factor out $\xi(w)$, defining

$$\hat{h}(w) = h(w)/\xi(w). \tag{13}$$

By virtue of Eq. (6), the $\overline{B} \to D l\bar{\nu}$ form factors only depend on two linear combinations of subleading Isgur-Wise functions, $\hat{L}_1$ and $\hat{L}_4$,

$$\begin{aligned}
\hat{h}_+ &= 1 + \hat{\alpha}_s\left[C_{V_1} + \frac{w+1}{2}(C_{V_2} + C_{V_3})\right] + (\varepsilon_c + \varepsilon_b)\hat{L}_1,\\
\hat{h}_- &= \hat{\alpha}_s\frac{w+1}{2}(C_{V_2} - C_{V_3}) + (\varepsilon_c - \varepsilon_b)\hat{L}_4,\\
\hat{h}_S &= 1 + \hat{\alpha}_s C_S + (\varepsilon_c + \varepsilon_b)\left(\hat{L}_1 - \hat{L}_4\frac{w-1}{w+1}\right),\\
\hat{h}_T &= 1 + \hat{\alpha}_s(C_{T_1} - C_{T_2} + C_{T_3}) + (\varepsilon_c + \varepsilon_b)(\hat{L}_1 - \hat{L}_4).
\end{aligned} \tag{14}$$

For the $\overline{B} \to D^* l\bar{\nu}$ form factors we obtain

[1] Our definitions of the subleading Isgur-Wise functions, $\chi_{1,2,3}$, $\eta$, and hence $\hat{L}_{1\ldots6}$, are dimensionless due to factoring out $\bar{\Lambda}$, as done, e.g., in Refs. [16,22] but not in Refs. [13,15]; the correspondence is obvious. The QCD sum rule calculations [23–25] also compute these functions with the dimensionless definitions.

$$
\begin{aligned}
\hat{h}_V &= 1+\hat{\alpha}_s C_{V_1}+\varepsilon_c(\hat{L}_2-\hat{L}_5)+\varepsilon_b(\hat{L}_1-\hat{L}_4),\\
\hat{h}_{A_1} &= 1+\hat{\alpha}_s C_{A_1}+\varepsilon_c\left(\hat{L}_2-\hat{L}_5\frac{w-1}{w+1}\right)\\
&\quad+\varepsilon_b\left(\hat{L}_1-\hat{L}_4\frac{w-1}{w+1}\right),\\
\hat{h}_{A_2} &= \hat{\alpha}_s C_{A_2}+\varepsilon_c(\hat{L}_3+\hat{L}_6),\\
\hat{h}_{A_3} &= 1+\hat{\alpha}_s(C_{A_1}+C_{A_3})+\varepsilon_c(\hat{L}_2-\hat{L}_3+\hat{L}_6-\hat{L}_5)\\
&\quad+\varepsilon_b(\hat{L}_1-\hat{L}_4),\\
\hat{h}_P &= 1+\hat{\alpha}_s C_P+\varepsilon_c[\hat{L}_2+\hat{L}_3(w-1)+\hat{L}_5-\hat{L}_6(w+1)]\\
&\quad+\varepsilon_b(\hat{L}_1-\hat{L}_4),\\
\hat{h}_{T_1} &= 1+\hat{\alpha}_s\left[C_{T_1}+\frac{w-1}{2}(C_{T_2}-C_{T_3})\right]+\varepsilon_c\hat{L}_2+\varepsilon_b\hat{L}_1,\\
\hat{h}_{T_2} &= \hat{\alpha}_s\frac{w+1}{2}(C_{T_2}+C_{T_3})+\varepsilon_c\hat{L}_5-\varepsilon_b\hat{L}_4,\\
\hat{h}_{T_3} &= \hat{\alpha}_s C_{T_2}+\varepsilon_c(\hat{L}_6-\hat{L}_3).
\end{aligned}
\tag{15}
$$

In Eqs. (14) and (15), the relations for the SM currents—that is, $h_+$, $h_-$, $h_V$, $h_{A_1}$, $h_{A_2}$, and $h_{A_3}$—agree with the literature, e.g., Refs. [16,20]. Because of Luke's theorem, the $\mathcal{O}(\Lambda_{\rm QCD}/m_{c,b})$ corrections to $h_+$, $h_S$, $h_{A_1}$, and $h_{T_1}$ vanish at zero recoil. To the best of our knowledge, the expressions for $h_T$ and $h_{T_{1,2,3}}$ cannot be found in the literature. For $h_{T_2}$ and $h_{T_3}$, which start at order $\Lambda_{\rm QCD}/m_{c,b}$, the partial results used in the literature (e.g., Ref. [28]) kept and left out terms, which are both order $\mathcal{O}(\Lambda_{\rm QCD}/m_{c,b})$.

The scalar and vector matrix elements in $\overline{B}\to D$ transitions, and the pseudoscalar and axial vector ones in $\overline{B}\to D^*$, are related by the equations of motion

$$
\begin{aligned}
[\overline{m}_b(\mu)-\overline{m}_c(\mu)]\langle D|\bar{c}b|\overline{B}\rangle &= \langle D|\bar{c}\not{q}b|\overline{B}\rangle,\\
-[\overline{m}_b(\mu)+\overline{m}_c(\mu)]\langle D^*|\bar{c}\gamma^5 b|\overline{B}\rangle &= \langle D^*|\bar{c}\not{q}\gamma^5 b|\overline{B}\rangle,
\end{aligned}
\tag{16}
$$

in which $\overline{m}_Q(\mu)$ are the $\overline{\rm MS}$ quark masses at a common scale $\mu$, obeying

$$
m_Q=\overline{m}_Q(\mu)\left[1+\hat{\alpha}_s\left(\frac{4}{3}-\ln\frac{m_Q^2}{\mu^2}\right)+\cdots\right]. \tag{17}
$$

One can verify using $m_b=m_B-\bar{\Lambda}+\mathcal{O}(\Lambda^2_{\rm QCD}/m_b)$ and $m_c=m_{D^{(*)}}-\bar{\Lambda}+\mathcal{O}(\Lambda^2_{\rm QCD}/m_c)$ that the form factor expansions in Eqs. (14) and (15) satisfy these relations, including all $\mathcal{O}(\varepsilon_{c,b})$ and $\mathcal{O}(\alpha_s)$ terms. We emphasize that this only holds using the $\overline{\rm MS}$ masses at the common scale $\mu$. Using $\overline{m}_b(\overline{m}_b)$ and $\overline{m}_c(\overline{m}_c)$ [29] in Eq. (16), as done in some papers, is inconsistent.

We prefer to evaluate the scalar and pseudoscalar matrix elements using Eqs. (14) and (15) instead of Eq. (16), because the natural choice for $\mu$ is below $m_b$ (or sometimes well below, as in the small-velocity limit [30,31]). In the $\overline{\rm MS}$ scheme fermions do not decouple for $\mu<m$, introducing artificially large corrections in the running, compensated by corresponding spurious terms in the $\beta$ function computed without integrating out heavy quarks [32].

### C. Decay rates and form factor ratios

The $\overline{B}\to D^{(*)}l\bar{\nu}$ differential rates have the well-known expressions in the SM,

$$
\begin{aligned}
\frac{{\rm d}\Gamma(\overline{B}\to Dl\bar{\nu})}{{\rm d}w} &= \frac{G_F^2|V_{cb}|^2\eta_{\rm EW}^2 m_B^5}{48\pi^3}(w^2-1)^{3/2}\\
&\quad\times r_D^3(1+r_D)^2\mathcal{G}(w)^2,
\end{aligned}
\tag{18a}
$$

$$
\begin{aligned}
\frac{{\rm d}\Gamma(\overline{B}\to D^*l\bar{\nu})}{{\rm d}w} &= \frac{G_F^2|V_{cb}|^2\eta_{\rm EW}^2 m_B^5}{48\pi^3}(w^2-1)^{1/2}(w+1)^2\\
&\quad\times r_{D^*}^3(1-r_{D^*})^2\\
&\quad\times\left[1+\frac{4w}{w+1}\frac{1-2wr_{D^*}+r_{D^*}^2}{(1-r_{D^*})^2}\right]\mathcal{F}(w)^2,
\end{aligned}
\tag{18b}
$$

where $r_{D^{(*)}}=m_{D^{(*)}}/m_B$ and $\eta_{\rm EW}\simeq 1.0066$ [33] is the electroweak correction. In addition,

$$
\mathcal{G}(w)=h_+-\frac{1-r_D}{1+r_D}h_-, \tag{19a}
$$

$$
\begin{aligned}
\mathcal{F}(w)^2 &= h_{A_1}^2\left\{2(1-2wr_{D^*}+r_{D^*}^2)\left(1+R_1\frac{w-1}{w+1}\right)\right.\\
&\quad\left.+[(1-r_{D^*})+(w-1)(1-R_2)]^2\right\}\\
&\quad\times\left[(1-r_{D^*})^2+\frac{4w}{w+1}(1-2wr_{D^*}+r_{D^*}^2)\right]^{-1},
\end{aligned}
\tag{19b}
$$

and the form-factor ratios are defined as

$$
R_1(w)=\frac{h_V}{h_{A_1}},\qquad R_2(w)=\frac{h_{A_3}+r_{D^*}h_{A_2}}{h_{A_1}}. \tag{20}
$$

In the heavy quark limit, $R_{1,2}(w)=1$ and $\mathcal{F}(w)=\mathcal{G}(w)=\xi(w)$, the leading Isgur-Wise function. It is common to fit the measured $\overline{B}\to D^*l\bar{\nu}$ angular distributions to $R_{1,2}(w)$. To $\mathcal{O}(\varepsilon_{c,b},\alpha_s)$, the SM predictions are

$$
\begin{aligned}
R_1(w) &= 1+\hat{\alpha}_s(C_{V_1}-C_{A_1})-\frac{2}{w+1}(\varepsilon_b\hat{L}_4+\varepsilon_c\hat{L}_5),\\
R_2(w) &= 1+\hat{\alpha}_s(C_{A_3}+r_{D^*}C_{A_2})-\frac{2}{w+1}(\varepsilon_b\hat{L}_4+\varepsilon_c\hat{L}_5)\\
&\quad+\varepsilon_c[\hat{L}_6(1+r_{D^*})-\hat{L}_3(1-r_{D^*})].
\end{aligned}
\tag{21}
$$

To include the lepton mass suppressed terms, one sometimes defines [28,34] additional form factor ratios

$$R_3(w) = \frac{h_{A_3} - r_{D^*} h_{A_2}}{h_{A_1}},$$
$$R_0(w) = \frac{h_{A_1}(w+1) - h_{A_3}(w - r_{D^*}) - h_{A_2}(1 - w r_{D^*})}{(1+r_{D^*}) h_{A_1}}. \quad (22)$$

All contributions of $R_{0,3}(w)$ are proportional to $m_\ell^2$. (The authors of Ref. [34] defined $R_3 = h_{A_3}/h_{A_1}$.) They are not linearly independent from $R_{1,2}(w)$, as there are only three form factor ratios in $B \to D^* \ell \bar{\nu}$ in the SM. In the heavy quark limit, $R_3(w) = R_0(w) = 1$. At $\mathcal{O}(\varepsilon_{c,b}, \alpha_s)$, the SM predictions are

$$\begin{aligned} R_3(w) &= 1 + \hat{\alpha}_s (C_{A_3} - r_{D^*} C_{A_2}) - \frac{2}{w+1}(\varepsilon_b \hat{L}_4 + \varepsilon_c \hat{L}_5) \\ &\quad + \varepsilon_c [\hat{L}_6 (1 - r_{D^*}) - \hat{L}_3 (1 + r_{D^*})], \\ R_0(w) &= 1 + \hat{\alpha}_s \frac{C_{A_3}(r_{D^*} - w) - (1 - r_{D^*} w) C_{A_2}}{1 + r_{D^*}} \\ &\quad + \frac{2(w - r_{D^*})}{(1+r_{D^*})(1+w)}(\varepsilon_b \hat{L}_4 + \varepsilon_c \hat{L}_5) \\ &\quad + \varepsilon_c \left[ \hat{L}_3 (w-1) - \hat{L}_6 (w+1) \frac{1 - r_{D^*}}{1 + r_{D^*}} \right]. \end{aligned} \quad (23)$$

### D. The 1$S$ scheme and numerical results

The $C_\Gamma$ coefficients defined in Eq. (9) are functions of $w$ and $z = m_c/m_b$, and thus depend on the quark masses. As is well known, the pole mass of a heavy quark contains a leading renormalon ambiguity of order $\Lambda_{\rm QCD}$, and so does the HQET parameter $\bar{\Lambda}$, as they are ill-defined beyond perturbation theory. The ambiguity is canceled by a corresponding ambiguity in the perturbation series, connected to the factorial growth of the coefficients of $\hat{\alpha}_s^n$ [35–39]. The cancellation comes about as a nonanalytic term connected to the asymptotic nature of the perturbation series, $e^{-c/\alpha_s(M)} \sim (\Lambda_{\rm QCD}/M)^{c\beta_0/(4\pi)}$, where $\beta_0 = (11 - 2n_f/3)$ is the first coefficient in the expansion of the $\beta$ function. For example, Eq. (21) implies at zero recoil, $R_1(1) \simeq 1 + 4\hat{\alpha}_s/3 + \varepsilon_c + \varepsilon_b - 2\varepsilon_b \eta(1)$, where the order $\hat{\alpha}_s{}^2 \beta_0$ terms are also known [22]. The leading renormalon corresponding to the worst behavior of the $\hat{\alpha}_s{}^n$ power series is canceled by the ambiguity in $\bar{\Lambda}$ within the $\varepsilon_c + \varepsilon_b$ term. The $-2\varepsilon_b \eta(1)$ term, however, does not contribute to this leading renormalon cancellation, as the only participating terms are those $\bar{\Lambda}/m_{c,b}$ terms not multiplied by any subleading Isgur-Wise functions.

The $\alpha_s$ perturbation series is known to be poorly convergent for many $B$ decay processes already at $\mathcal{O}(\alpha_s^2)$, when expressed in terms of the pole mass. To ensure the order-by-order cancellation of the fastest factorially growing terms, it is convenient to reorganize the perturbation series in terms of a suitable short-distance mass scheme, instead of the pole mass. We use the 1$S$ scheme [40–42], which has been tested in the calculations of numerous observables. (Using the $\overline{\rm MS}$ mass yields a poorly behaved perturbation series, for the reasons mentioned at the end of Sec. II B. Other possible short-distance mass schemes include the potential-subtracted (PS) mass [43] or the kinetic mass [44].)

The 1$S$ scheme defines $m_b^{1S}$ as half of the perturbatively computed $\Upsilon(1S)$ mass. It is related to the pole mass as $m_b^{1S} = m_b(1 - 2\alpha_s^2/9 + \cdots)$ [40–42], so that we may treat the pole mass as the function $m_b(m_b^{1S}) = m_b^{1S}(1 + 2\alpha_s^2/9 + \cdots)$. Neglecting higher-order terms, as done throughout this paper, is a good approximation in all cases where they are known, including the evaluation of $R_{1,2}$ [22]. We adopt the inputs [45],

$$\begin{aligned} m_b^{1S} &= (4.71 \pm 0.05)\ \text{GeV}, \\ \delta m_{bc} &= m_b - m_c = (3.40 \pm 0.02)\ \text{GeV}, \end{aligned} \quad (24)$$

from fits to inclusive $B \to X_c l \bar{\nu}$ spectra and other determinations of $m_b^{1S}$. We eliminate $m_c$ using $m_c = m_b(m_b^{1S}) - \delta m_{bc}$, and extract $\bar{\Lambda}$ via

$$\bar{\Lambda} = \overline{m}_B - m_b(m_b^{1S}) + \lambda_1/(2m_b^{1S}). \quad (25)$$

Here $\overline{m}_B = (m_B + 3m_{B^*})/4 \simeq 5.313$ GeV is the spin-averaged meson mass, and we use $\lambda_1 = -0.3$ GeV$^2$ [45]. Enforcing the cancellation of the leading renormalon is equivalent to using $m_b(m_b^{1S}) \to m_b^{1S}$ everywhere in Eqs. (14) and (15), except in the $\bar{\Lambda}/m_{c,b}$ terms that are not multiplied by subleading Isgur-Wise functions.

We match the QCD and HQET theories at the scale $\mu^2 = m_b m_c$, corresponding to $\alpha_s \simeq 0.26$. The 1$S$ scheme then yields, for example, the following SM predictions for $R_{1,2}(1)$:

$$\begin{aligned} R_1(1) &\simeq 1.34 - 0.12\eta(1), \\ R_2(1) &\simeq 0.98 - 0.42\eta(1) - 0.54\hat{\chi}_2(1). \end{aligned} \quad (26)$$

For $R'_{1,2}(1)$ we obtain

$$\begin{aligned} R'_1(1) &\simeq -0.15 + 0.06\eta(1) - 0.12\eta'(1), \\ R'_2(1) &\simeq 0.01 - 0.54\hat{\chi}'_2(1) + 0.21\eta(1) - 0.42\eta'(1). \end{aligned} \quad (27)$$

For completeness, the similar relations for $R_{0,3}$ are

$$R_3(1) \simeq 1.19 - 0.26\eta(1) - 1.20\hat{\chi}_2(1),$$
$$R_0(1) \simeq 1.09 + 0.25\eta(1),$$
$$R_3'(1) \simeq -0.08 - 1.20\hat{\chi}_2'(1) + 0.13\eta(1) - 0.26\eta'(1),$$
$$R_0'(1) \simeq -0.18 + 0.87\hat{\chi}_2(1) + 0.06\eta(1) + 0.25\eta'(1). \quad (28)$$

## III. COMBINED FIT TO $B \to D^* l\bar{\nu}$ AND $B \to Dl\bar{\nu}$

### A. Parametrization of the $w$ dependence

Unitarity and analyticity provide strong constraints on the shapes of the $\overline{B} \to D^{(*)}\ell\bar{\nu}$ form factors [46–51]. It is common to employ a parametrization of the $\overline{B} \to D\ell\bar{\nu}$ form factor $\mathcal{G}(w)$, defined in Eq. (19), via the conformal mapping $z(w) = (\sqrt{w+1} - \sqrt{2})/(\sqrt{w+1} + \sqrt{2})$. Unitarity constraints yield, e.g., $\mathcal{G}(w)/\mathcal{G}(1) \simeq 1 - 8\rho^2 z + (51.\rho^2 - 10.)z^2 - (252.\rho^2 - 84.)z^3$, in which $\rho^2 = -\mathcal{G}'(1)/\mathcal{G}(1)$ is a slope parameter [48]. The convergence of this expansion may be optimized by parametrizing it in a way that minimizes the range of the expansion parameter, via

$$z_*(w) = \frac{\sqrt{w+1} - \sqrt{2}a}{\sqrt{w+1} + \sqrt{2}a}, \qquad a = \left(\frac{1+r_D}{2\sqrt{r_D}}\right)^{1/2}. \quad (29)$$

For $\overline{B} \to Dl\bar{\nu}$, $|z_*| \leq 0.032$. The unitarity constraints suggest a form factor parametrization of the form

$$\frac{\mathcal{G}(w)}{\mathcal{G}(w_0)} \simeq 1 - 8a^2\rho_*^2 z_* + (V_{21}\rho_*^2 - V_{20})z_*^2. \quad (30)$$

Here $w_0 = 2a^2 - 1 \simeq 1.28$ is defined such that $z_*(w_0) = 0$, while $V_{21} \simeq 57.$ and $V_{20} \simeq 7.5$ are obtained numerically from Ref. [48]. The uncertainty in the coefficient of the $z_*^2$ term in Eq. (30) may be sizable [48]. However, the impact of this term on the physical fit results is expected to be small.

The leading-order Isgur-Wise function, $\xi(w)$, may be extracted from the parametrization in Eq. (30) by using Eqs. (14) and (13). Keeping terms to $\mathcal{O}(\varepsilon_{c,b}(w-1))$, we can approximate the subleading Isgur-Wise functions as

$$\hat{\chi}_2(w) \simeq \hat{\chi}_2(1) + \hat{\chi}_2'(1)(w-1), \qquad \hat{\chi}_3(w) \simeq \hat{\chi}_3'(1)(w-1),$$
$$\eta(w) \simeq \eta(1) + \eta'(1)(w-1), \quad (31)$$

since $\hat{\chi}_3(1) = 0$. One finds at $\mathcal{O}(\varepsilon_{c,b}, \alpha_s)$,

$$\begin{aligned}\frac{\xi(w)}{\xi(w_0)} \simeq 1 &- 8a^2\bar{\rho}_*^2 z_* + z_*^2\Bigg\{V_{21}\bar{\rho}_*^2 - V_{20} + (\varepsilon_b - \varepsilon_c)\left[2\Xi\eta'(1)\frac{1-r_D}{1+r_D}\right] \\ &+ (\varepsilon_b + \varepsilon_c)\left[\Xi[12\hat{\chi}_3'(1) - 4\hat{\chi}_2(1)] - 16[(a^2-1)\Xi - 16a^4]\hat{\chi}_2'(1)\right] \\ &+ \hat{\alpha}_s\Bigg[\Xi\left(C_{V_1}'(w_0) + \frac{C_{V_3}(w_0) + r_D C_{V_2}(w_0)}{1+r_D}\right) + 2a^2(\Xi - 32a^2)\frac{C_{V_3}'(w_0) + r_D C_{V_2}'(w_0)}{1+r_D} \\ &- 64a^6\frac{C_{V_3}''(w_0) + r_D C_{V_2}''(w_0)}{1+r_D} - 32a^4 C_{V_1}''(w_0)\Bigg]\Bigg\}, \end{aligned} \quad (32)$$

where $\Xi = 64a^4\bar{\rho}_*^2 - 16a^2 - V_{21}$. The slope parameter $\bar{\rho}_*^2 = -\xi'(w_0)/\xi(w_0)$ is related to the slope $\rho_*^2 = -\mathcal{G}'(w_0)/\mathcal{G}(w_0)$ via

$$\begin{aligned}\bar{\rho}_*^2 - \rho_*^2 = &(\varepsilon_b + \varepsilon_c)\left[12\hat{\chi}_3'(1) - 4\hat{\chi}_2(1) - 16(a^2-1)\hat{\chi}_2'(1)\right] \\ &+ 2(\varepsilon_b - \varepsilon_c)\eta'(1)\frac{1-r_D}{1+r_D} \\ &+ \hat{\alpha}_s\Bigg[\frac{r_D C_{V_2}(w_0) + C_{V_3}(w_0)}{1+r_D} + C_{V_1}'(w_0) \\ &+ 2a^2\frac{r_D C_{V_2}'(w_0) + C_{V_3}'(w_0)}{1+r_D}\Bigg]. \end{aligned} \quad (33)$$

Enforcing $\xi(1) = 1$, one may directly extract $\xi(w_0)$ via evaluation of Eq. (32) at the zero recoil point, $z_*(w=1) = (1-a)/(1+a)$, and thereby obtain a properly normalized parametrization for $\xi(w)$. Since $\eta(1)$ does not appear in Eq. (32), this implies that constraining $\xi(w)$ in itself does not constrain $\eta(1)$, which is the largest unknown contribution in $R_{1,2}(1)$.

This expression for $\xi(w)$, combined with the HQET expansions in Eqs. (14) and (15), allows one to parametrize all $\overline{B} \to D^{(*)}$ form factors in terms of six parameters: $\bar{\rho}_*^2$, $\hat{\chi}_2(1)$, $\hat{\chi}_2'(1)$, $\hat{\chi}_3'(1)$, $\eta(1)$ and $\eta'(1)$. The normalizations of the form factors are also fixed by Eq. (32), and thus $|V_{cb}|$ may be determined from a global fit to overall rates without using lattice results.

### B. QCD sum rule inputs

The subleading Isgur-Wise functions have only been calculated using model-dependent methods, and are not yet available from lattice QCD. The two-loop QCD sum rule (QCDSR) calculations [23–25] imply that the subleading Isgur-Wise function $\eta(w)$ is approximately constant. The functions $\hat{\chi}_{2,3}$, which parametrize corrections

from the chromomagnetic term in the subleading HQET Lagrangian, are small, in agreement with quark model intuition.

The QCD sum rule results are obtained at a fixed scale. The scale dependence can be removed from $\hat{\chi}_{2,3}$ by defining "renormalization improved" functions, $\hat{\chi}^{\rm ren}_{2,3}$ [16]. These are obtained by multiplying the results of Refs. [23,24] for $\hat{\chi}_{2,3}$ by $[\alpha_s(\Lambda)]^{3/\beta_0} \sim 1.4$, where $\Lambda \sim 1$ GeV and $\beta_0 = 9$ for three light flavors. For these renormalized subleading Isgur-Wise functions, we use

$$\begin{aligned} &\hat{\chi}_2^{\rm ren}(1) = -0.06 \pm 0.02, \qquad \hat{\chi}_2'^{\rm ren}(1) = 0 \pm 0.02, \\ &\hat{\chi}_3'^{\rm ren}(1) = 0.04 \pm 0.02, \qquad \eta(1) = 0.62 \pm 0.2, \\ &\eta'(1) = 0 \pm 0.2. \end{aligned} \tag{34}$$

These central values reproduce $\hat{L}_{1\ldots6}$ in Ref. [48], often used to predict $R_{1,2}$ and $R(D^{(*)})$.

We assign relatively large uncertainties, to permit assessment of possible pulls of the experimental data from these QCDSR predictions. Replacing $\hat{\chi}_{2,3}$ with $\hat{\chi}^{\rm ren}_{2,3}$, the Wilson coefficient of the chromomagnetic operator receives a corresponding $\alpha_s(\mu)^{3/\beta_0}$ factor at the matching scale $\mu = \sqrt{m_b m_c}$, partly canceling the above $[\alpha_s(\Lambda)]^{3/\beta_0}$ enhancement. For ease of comparison with the literature we ignore this, as it can be viewed as a higher-order correction, and is in any case covered by the large assigned uncertainties. We ignore correlations in the QCDSR results (arising from the common calculational method), which is conservative.

Using Eq. (34) in Eq. (21) yields expressions for $R_{1,2}(w)$ as polynomials in $(w-1)$, with the coefficients and their uncertainties correlated by HQET. In Ref. [48], the central values in Eq. (34) were used to write $R_{1,2}(w)$ as quadratic polynomials, without quoting any theory uncertainties on their slopes and curvatures. It subsequently become standard practice in experimental $|V_{cb}|$ and $R_{1,2}$ measurements to fit for $R_{1,2}(1)$, while fixing $R'_{1,2}(1)$ and $R''_{1,2}(1)$ to their quoted central values [48]. Such an approach is inconsistent with the simultaneous use of the HQET constraints and the QCDSR results. For example, the present world average central value, $R_1(1) \simeq 1.4$, cannot simultaneously satisfy the HQET prediction for $R_1(1)$ in Eq. (26) and the QCDSR expectation $\eta(1) > 0$, which holds at the $3\sigma$ level, and is used elsewhere in the same fit. A consistent treatment of these form factor ratios is absent from the derivations of the state-of-the-art predictions for $R(D^{(*)})$ in the SM [except for lattice QCD (LQCD) $R(D)$ predictions] and in the presence of new physics [28,34].

We now proceed to assess the importance of obeying the HQET relations between different form factors, and of including the uncertainties in the QCDSR predictions in Eq. (34). These effects will be important in the future, to systematically improve the SM predictions.

### C. Fit scenarios

A simultaneous fit of the six parameters $\bar{\rho}^2_*, \hat{\chi}_2(1), \hat{\chi}'_2(1), \hat{\chi}'_3(1), \eta(1)$, and $\eta'(1)$ to the $\overline{B} \to D^{(*)} l\bar{\nu}$ rates can be carried out with the present data. Such a fit fixes both the shapes and normalizations of the $\overline{B} \to D^{(*)} l\bar{\nu}$ rates, without any theory input other than the HQET expansion. However, one expects large uncertainties at present, because of the limited experimental precision and the number of subleading HQET parameters. One may instead use QCD sum rule predictions and/or lattice QCD results to constrain the fit, increasing sensitivity to $\bar{\rho}^2_*$. The fit propagates the uncertainties on the subleading Isgur-Wise functions into the fit result, and allows the data to further constrain the subleading contributions.

Our fit relies on the HQET predictions and unitarity constraints to determine the ratios and shapes of the form factors. The form factors at zero recoil, $\mathcal{G}(1)$ and $\mathcal{F}(1)$, have been computed in LQCD, providing state-of-the-art predictions for the normalizations of the $\overline{B} \to D^{(*)} l\bar{\nu}$ rates. The most precise lattice QCD predictions at zero recoil are [52,53]

$$\mathcal{G}(1)_{\rm LQCD} = 1.054(8), \quad \mathcal{F}(1)_{\rm LQCD} = 0.906(13), \tag{35}$$

where we combined the quoted systematic and statistical uncertainties. Although these normalizations may be expected to drop out of the predictions for $R(D^{(*)})$, they do influence the fit to the differential decay distributions and hence the resulting form factor ratios. Making use of these lattice constraints leads to our first fitting scenario:

(i) Rescale the $\overline{B} \to D$ and $\overline{B} \to D^*$ form factors in the fit by $\mathcal{G}(1)_{\rm LQCD}/\mathcal{G}(1)$ and $\mathcal{F}(1)_{\rm LQCD}/\mathcal{F}(1)$, respectively, such that the rates at $w = 1$ agree with the lattice predictions. We refer to this fit as "$\rm L_{w=1}$."

Measurements of the rate normalizations are, however, subject to relatively large systematic uncertainties. For example, the calibration of the hadronic tagging efficiency produces systematic uncertainties of the order of a few percent [54]. To compare the best-fit shapes without lattice constraints and such systematic effects, we consider a second scenario:

(ii) Allow the normalizations of the $\overline{B} \to D l\bar{\nu}$ and $\overline{B} \to D^* l\bar{\nu}$ rates to float independently. This approach only uses $\overline{B} \to D^{(*)} l\bar{\nu}$ shape information to constrain the form factors, but no theory input for the normalizations at zero recoil, and is independent of lattice information. We refer to this fit as "NoL."

For each fit, we apply (relax) the QCDSR constraints, exploring a "constrained" ("unconstrained") fit. The QCDSR constrained fits are denoted with a suffix "+SR." Both $\rm L_{w=1}$ and NoL fits alter the overall normalizations the $\overline{B} \to D l\bar{\nu}$ and $\overline{B} \to D^* l\bar{\nu}$ rates, but leave the HQET expansions of the form factors unchanged. Thus, they can be considered as introducing an extra source of

heavy quark symmetry breaking in the normalizations (to effectively account for higher-order effects), while still preserving the form factor relations independently in Eqs. (14) and (15).

Since lattice QCD predictions are also available for $w \geq 1$ for the $\overline{B} \to D l \bar{\nu}$ form factors $f_+(w)$ and $f_0(w)$, it is possible to obtain a prediction for the slope parameter, $\bar{\rho}^2_*$, from them. This leads to a third fit approach, namely:

(iii) Extract $\xi(w)$, including the slope parameter $\bar{\rho}^2_*$, by fitting to the $w \geq 1$ lattice QCD data for $B \to D$, and apply it simultaneously with the LQCD normalization of $B \to D^*$ at $w = 1$. We refer to this fit as "$\mathrm{L}_{w\geq 1}$."

In a "theory only" version of this fit, denoted by "$\mathrm{th}:\mathrm{L}_{w\geq 1} + \mathrm{SR}$," one fully constrains the $\overline{B} \to D^{(*)} l \bar{\nu}$ differential rates without any experimental input; the only fit is to lattice data and QCDSR constraints. For the "$\mathrm{L}_{w\geq 1} + \mathrm{SR}$" fit, we combine the $w \geq 1$ $B \to D$ and $w = 1$ $B \to D^*$ lattice data with QCDSR constraints and the experimental information, to include all available information and explore possible tensions. We summarize the inputs of the various fit scenarios pursued in this paper in Table I.

TABLE I. Summary of theory and data inputs for each fit scenario. All use the HQET predictions to order $\mathcal{O}(\Lambda_{\mathrm{QCD}}/m_{c,b})$ and $\mathcal{O}(\alpha_s)$, as well as the unitarity constraints.

| | | Lattice QCD | | | |
|---|---|---|---|---|---|
| Fit | QCDSR | $\mathcal{F}(1)$ | $f_{+,0}(1)$ | $f_{+,0}(w>1)$ | Belle Data |
| $\mathrm{L}_{w=1}$ | ... | ✓ | ✓ | ... | ✓ |
| $\mathrm{L}_{w=1} + \mathrm{SR}$ | ✓ | ✓ | ✓ | ... | ✓ |
| NoL | ... | ... | ... | ... | ✓ |
| NoL + SR | ✓ | ... | ... | ... | ✓ |
| $\mathrm{L}_{w\geq 1}$ | ... | ✓ | ✓ | ✓ | ✓ |
| $\mathrm{L}_{w\geq 1} + \mathrm{SR}$ | ✓ | ✓ | ✓ | ✓ | ✓ |
| $\mathrm{th}:\mathrm{L}_{w\geq 1} + \mathrm{SR}$ | ✓ | ✓ | ✓ | ✓ | ... |

All fits explored in this paper use the unitarity constraints. The consequences of relaxing the unitarity constraints between the slope and the curvature terms in Eq. (30) will be explored in detail elsewhere [55].

### D. Data and fit details

To determine the leading and subleading Isgur-Wise functions and $|V_{cb}|$, we carry out a simultaneous fit of the available $\overline{B} \to D^{(*)} l \bar{\nu}$ spectra. There are only two measurements [54,56] which provide kinematic distributions fully corrected for detector effects. The measured recoil and decay angle distributions are analyzed simultaneously by constructing a standard $\chi^2$ function. Common uncertainties (tagging efficiency, reconstruction efficiencies, number of $B$-meson pairs) should be treated as fully correlated between the two measurements and we construct a covariance using Table IV in Ref. [56] and Table IV in Ref. [54]. While Ref. [56] provides a full breakdown of the total uncertainty for each measured $w$ bin, Ref. [54] only provides a breakdown for the total branching fraction. To construct the desired covariance between both measurements, we thus assume that there is no shape dependence on the tagging and reconstruction efficiency uncertainty of Ref. [54]. Comparing this with the mild dependence on these error sources in Ref. [56], this seems a fair approximation of the actual covariance. To take into account the uncertainties of $m_b^{1S}$ and $\delta m_{bc}$, we introduce both as nuisance parameters into the fit, assuming Gaussian constraints with uncertainties given in Eq. (24). The $\chi^2$ function is numerically minimized and uncertainties are evaluated using the usual asymptotic approximations by scanning the $\Delta\chi^2 = \chi^2_{\mathrm{scan}} - \chi^2_{\mathrm{min}}$ contour to find the $+1$ crossing point, which provides the 68% confidence level. The constraints from lattice QCD predictions and/or QCD sum rules are incorporated into the fit assuming (multivariate) Gaussian errors and are added to the $\chi^2$ function.

TABLE II. Summary of the results for the fit scenarios considered. The correlations are shown in Appendix B.

| | $\mathrm{L}_{w=1}$ | $\mathrm{L}_{w=1} + \mathrm{SR}$ | NoL | NoL + SR | $\mathrm{L}_{w\geq 1}$ | $\mathrm{L}_{w\geq 1} + \mathrm{SR}$ | $\mathrm{th}:\mathrm{L}_{w\geq 1} + \mathrm{SR}$ |
|---|---|---|---|---|---|---|---|
| $\chi^2$ | 40.2 | 44.0 | 38.7 | 43.1 | 49.0 | 53.8 | 7.4 |
| dof | 44 | 48 | 43 | 47 | 48 | 52 | 4 |
| $\lvert V_{cb}\rvert \times 10^3$ | $38.8 \pm 1.2$ | $38.5 \pm 1.1$ | ... | ... | $39.1 \pm 1.1$ | $39.3 \pm 1.0$ | ... |
| $\mathcal{G}(1)$ | $1.055 \pm 0.008$ | $1.056 \pm 0.008$ | ... | ... | $1.060 \pm 0.008$ | $1.061 \pm 0.007$ | $1.052 \pm 0.008$ |
| $\mathcal{F}(1)$ | $0.904 \pm 0.012$ | $0.901 \pm 0.011$ | ... | ... | $0.898 \pm 0.012$ | $0.895 \pm 0.011$ | $0.906 \pm 0.013$ |
| $\bar{\rho}^2_*$ | $1.17 \pm 0.12$ | $1.19 \pm 0.07$ | $1.06 \pm 0.15$ | $1.19 \pm 0.08$ | $1.33 \pm 0.11$ | $1.24 \pm 0.06$ | $1.24 \pm 0.08$ |
| $\hat{\chi}_2(1)$ | $-0.26 \pm 0.26$ | $-0.07 \pm 0.02$ | $0.36 \pm 0.62$ | $-0.06 \pm 0.02$ | $0.13 \pm 0.22$ | $-0.06 \pm 0.02$ | $-0.06 \pm 0.02$ |
| $\hat{\chi}'_2(1)$ | $0.21 \pm 0.38$ | $-0.00 \pm 0.02$ | $0.14 \pm 0.39$ | $-0.00 \pm 0.02$ | $-0.36 \pm 0.28$ | $-0.00 \pm 0.02$ | $-0.00 \pm 0.02$ |
| $\hat{\chi}'_3(1)$ | $0.02 \pm 0.07$ | $0.05 \pm 0.02$ | $0.18 \pm 0.19$ | $0.04 \pm 0.02$ | $0.09 \pm 0.07$ | $0.05 \pm 0.02$ | $0.04 \pm 0.02$ |
| $\eta(1)$ | $0.30 \pm 0.04$ | $0.30 \pm 0.03$ | $-0.56 \pm 0.80$ | $0.35 \pm 0.14$ | $0.30 \pm 0.04$ | $0.30 \pm 0.03$ | $0.31 \pm 0.04$ |
| $\eta'(1)$ | 0 (fixed) | $-0.12 \pm 0.16$ | 0 (fixed) | $-0.11 \pm 0.18$ | 0 (fixed) | $-0.05 \pm 0.09$ | $0.05 \pm 0.10$ |
| $m_b^{1S}$ [GeV] | $4.70 \pm 0.05$ | $4.70 \pm 0.05$ | $4.71 \pm 0.05$ | $4.70 \pm 0.05$ | $4.71 \pm 0.05$ | $4.71 \pm 0.05$ | $4.71 \pm 0.05$ |
| $\delta m_{bc}$ [GeV] | $3.40 \pm 0.02$ | $3.40 \pm 0.02$ | $3.40 \pm 0.02$ | $3.40 \pm 0.02$ | $3.40 \pm 0.02$ | $3.40 \pm 0.02$ | $3.40 \pm 0.02$ |

The full fit results are shown in Table II. The "$L_{w=1}$" unconstrained fit, i.e., using only the lattice normalizations at $w = 1$, yields

$$|V_{cb}| = (38.8 \pm 1.2) \times 10^{-3}, \tag{36}$$

to be compared with the current world average [29] $|V_{cb}| = (42.2 \pm 0.8) \times 10^{-3}$ and $|V_{cb}| = (39.2 \pm 0.7) \times 10^{-3}$, from inclusive and exclusive $b \to c l \bar{\nu}_l$ decays, respectively. The uncertainties of the subleading Isgur-Wise parameters are sizable. There is no sensitivity to disentangle $\eta'(1)$ from $\bar{\rho}_*^2$, so we fix $\eta'(1)$ to be zero for all QCDSR unconstrained fits. Including the QCDSR constraints in the "$L_{w=1}$ + SR" fit yields

$$|V_{cb}| = (38.5 \pm 1.1) \times 10^{-3}, \tag{37}$$

resulting in almost the same $|V_{cb}|$ value. The normalization of $\eta(1)$ is comparable between these two fits, at about half the value of the QCDSR expectation. Both fits have reasonable $\chi^2$ values, corresponding to fit probabilities of 64% each.

Neglecting all subleading $\Lambda_{\rm QCD}/m_{c,b}$ contributions in the "$L_{w=1}$" fit results in a poorer overall $\chi^2$. The value of $|V_{cb}|$ decreases slightly, $|V_{cb}| = (38.2 \pm 1.1) \times 10^{-3}$, with $\chi^2 = 62.6$ for 48 d.o.f., corresponding to a fit probability of 8%, which is still an acceptable fit. The slope parameter becomes $\bar{\rho}_*^2 = 0.93 \pm 0.05$, below those obtained including the $\Lambda_{\rm QCD}/m_{c,b}$ corrections. The uncertainty of $\bar{\rho}_*^2$ is noticeably smaller due to the smaller number of degrees of freedom in this fit. The value of $|V_{cb}|$ is only weakly affected by this shift in $\bar{\rho}_*^2$.

In the "NoL" fits, using no LQCD inputs, we use only shape information to disentangle $\bar{\rho}_*^2$ from the subleading contributions, while allowing the $\overline{B} \to D l \bar{\nu}$ and $\overline{B} \to D^* l \bar{\nu}$ channels to each have arbitrary normalizations (these fits cannot determine $|V_{cb}|$). This results in large uncertainties in the QCDSR unconstrained fit. Again, $\eta'(1)$ and $\bar{\rho}_*^2$ are strongly correlated, so the former is fixed at zero. Including the QCDSR constraints in the "NoL + SR" fit yields results close to those in the "$L_{w=1}$ + SR" fit.

In the "th:$L_{w\geq 1}$ + SR" scenario, which uses no experimental data, fitting the parametrized $\xi(w)$ to the six lattice points for $f_{+,0}(w)$ in Table III and $\mathcal{F}(1)$ in Eq. (35), results in a slope parameter

$$\bar{\rho}_*^2 = 1.24 \pm 0.08. \tag{38}$$

The fitted $w$ spectra are shown in Fig. 1 (gray curves), together with the lattice data points. The $\chi^2$ of the fit is 7.4, corresponding to a fit probability of 11% with $7 - 3 = 4$ degrees of freedom. The value for the slope is in good agreement with the slope obtained from the QCDSR constrained and unconstrained "$L_{w=1}$" and "NoL" fits.

In the "$L_{w\geq 1}$" fit, all six lattice points for $f_{+,0}(w)$ in Table III and $\mathcal{F}(1)$ in Eq. (35) are fitted together with the available experimental information. Once again, $\eta'(1)$ is fixed to zero, as it is strongly correlated with $\bar{\rho}_*^2$. The fit has $\chi^2 = 49$, corresponding to a fit probability of 43%. For $|V_{cb}|$, this fit yields

$$|V_{cb}| = (39.1 \pm 1.1) \times 10^{-3}, \tag{39}$$

which is slightly higher than the "$L_{w=1}$" result. The value of $\bar{\rho}_*^2$ is also higher.

In the "$L_{w\geq 1}$ + SR" fit, the QCDSR constraints are included, so that all theory and experimental information is incorporated. The resulting differential $\overline{B} \to D^{(*)} l \bar{\nu}$ distributions are shown in Fig. 2, overlaid with the experimental data, as well as the predictions for the $\overline{B} \to D^{(*)} \tau \bar{\nu}$ differential rates. The fit has $\chi^2 = 53.8$, corresponding to a fit probability of 44%. For $|V_{cb}|$ the fit gives

$$|V_{cb}| = (39.3 \pm 1.0) \times 10^{-3}. \tag{40}$$

This is higher than the "$L_{w=1}$ + SR" result, because the value of $\bar{\rho}_*^2$ is also higher.

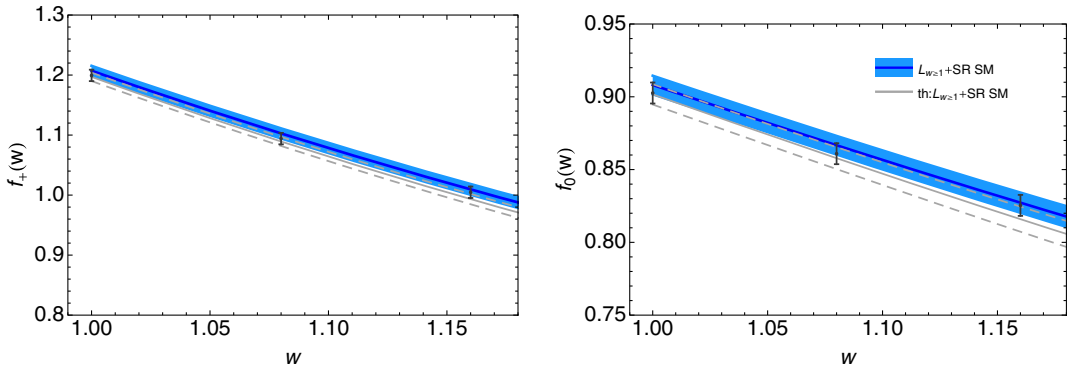


FIG. 1. The "th:$L_{w\geq 1}$ + SR" fit of the form factors $f_{+,0}$ to the lattice points listed in Table III is shown (gray solid line). The dashed gray lines correspond to the 68% errors. The dark blue line shows the $f_{+,0}$ best fit for "$L_{w\geq 1}$ + SR", using lattice points, experimental information, and QCDSR constraints. The blue band displays the corresponding 68% C.L. of this fit.

TABLE III. The predictions for the form factors $f_{+,0}$ at $w = 1.0, 1.08, 1.16$ using the synthetic data results of Ref. [53]. The correlations can be found in Table VII in Ref. [53].

| Form factor | $w = 1.0$ | $w = 1.08$ | $w = 1.16$ |
|---|---|---|---|
| $f_+$ | $1.1994 \pm 0.0095$ | $1.0941 \pm 0.0104$ | $1.0047 \pm 0.0123$ |
| $f_0$ | $0.9026 \pm 0.0072$ | $0.8609 \pm 0.0077$ | $0.8254 \pm 0.0094$ |

The correlation matrices for all fits are shown in Appendix B. In the "$L_{w=1}$" and "$L_{w\geq 1}$" type fits, moderate correlations are seen between $|V_{cb}|$, $\mathcal{G}(1)$, and $\mathcal{F}(1)$, as expected. The correlations are sizable in these fits between $\bar{\rho}_*^2$ and the subleading Isgur-Wise functions.

A more detailed study of these effects, in particular the extraction of $|V_{cb}|$, will be presented elsewhere [55]. A first comparison with the Caprini-Lellouch-Neubert (CLN) parametrization [48], as implemented by previous experimental studies, can be done by considering the results for the form factor ratios $R_1$ and $R_2$, defined in Eq. (20). Figure 3 shows the extracted values of $R_{1,2}(1)$ for all fit scenarios. The results agree with each other and with the world average of $R_1(1)$ and $R_2(1)$ [9] shown by black ellipses, up to a mild $1\sigma$ tension. Firm conclusions are difficult to reach, as it is impossible to assess how the experimental results would change, had the uncertainties in the quadratic polynomials used to fit $R_{1,2}(w)$ been properly included. When the QCDSR constraints are used, the

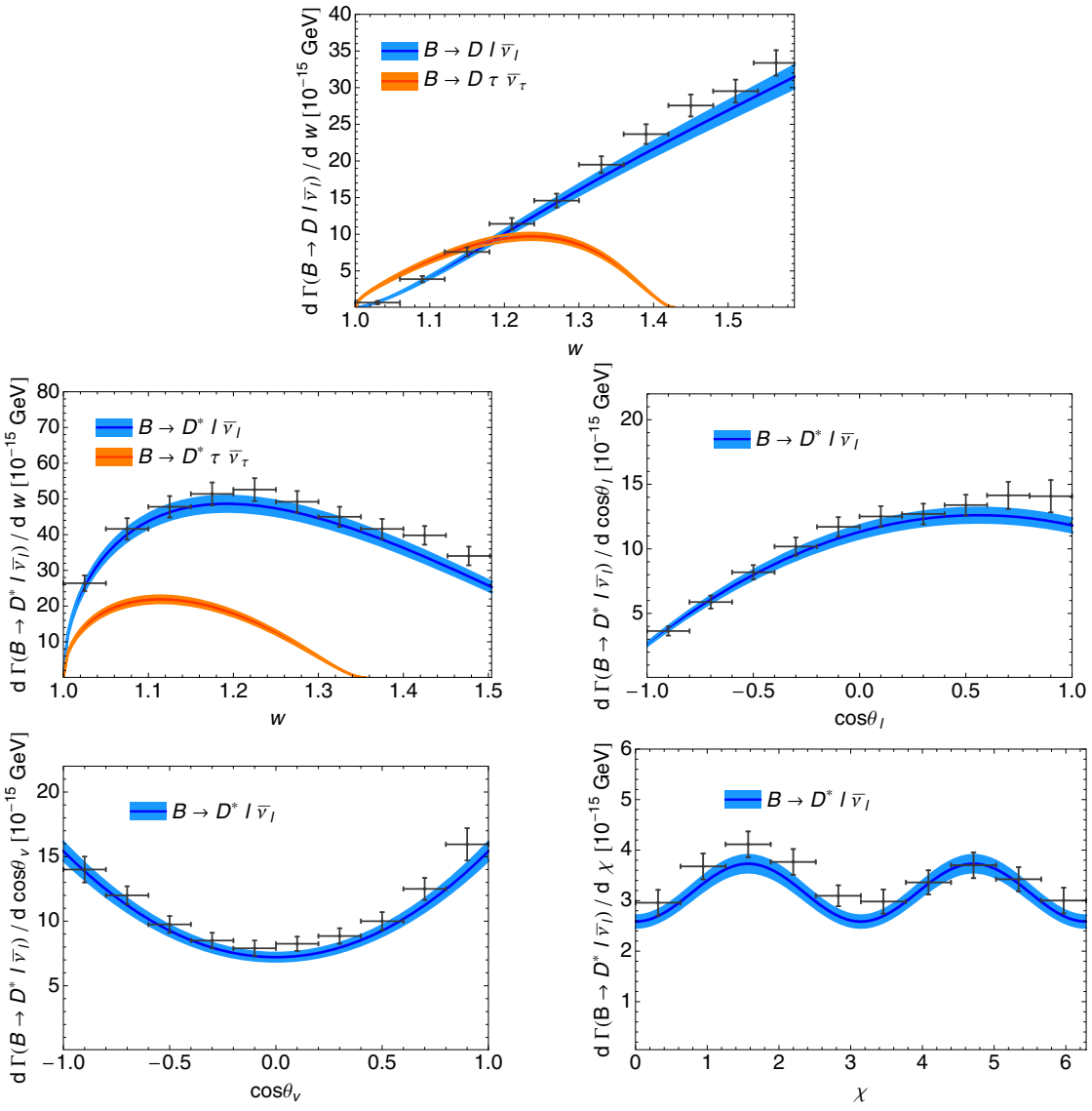


FIG. 2. The measured $\bar{B} \to D^{(*)} l \bar{\nu}$ decay distributions [54,56] compared to the best-fit contours (dark blue curves) for the "$L_{w\geq 1}$ + SR" fit, using LQCD at all $w$ and QCDSR constraints. The blue bands show the 68% C.L. regions. The orange curves and bands show the central values and the 68% C.L. regions of the fit predictions for $d\Gamma(\bar{B} \to D^{(*)} \tau \bar{\nu})/dw$.

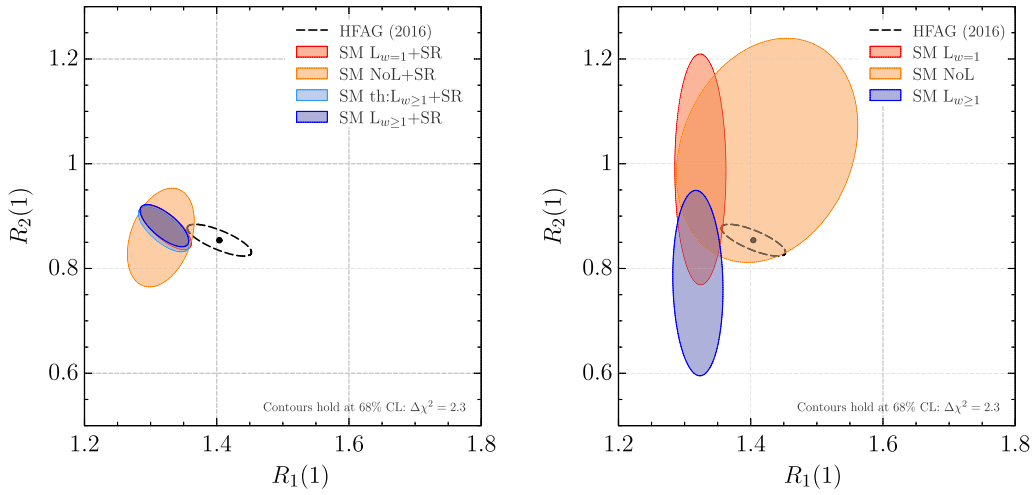


FIG. 3. The SM predictions for $R_1(1)$ and $R_2(1)$ for the fits imposing (left) or not imposing (right) the QCDSR constraints in Eq. (34). The black ellipse shows the world average of the data [9]. The fit scenarios are described in the text and in Table I, and the fit results are shown in Table II. All contours correspond to 68% C.L. in two dimensions ($\Delta\chi^2 = \chi^2_{\rm scan} - \chi^2_{\rm min} = 2.3$).

central values satisfy $R_1(1) < 1.34$, as required by the HQET prediction in Eq. (26) and the constraint $\eta(1) > 0$.

### E. $R(D^{(*)})$ and new physics

Using the fitted values for $\bar{\rho}^2_*$, $\hat{\chi}_2(1)$, $\hat{\chi}'_2(1)$, $\hat{\chi}'_3(1)$, $\eta(1)$, and $\eta'(1)$, one can predict $R(D^{(*)})$ in the SM and for any new physics four-fermion interaction. Figure 4 and Table IV summarize the predicted values of $R(D^{(*)})$ in the SM for the seven fit scenarios considered. Our fit results for $R(D)$ are in good agreement with other predictions in the literature [57,58]. All our fits using lattice QCD inputs yield $R(D^*)$ above those in Ref. [34]. This slightly eases the disagreement with the world average measurement [9]. The significance is calculated from $\chi^2$ statistics, taking into account the full covariance of the theory prediction and the world average measurement. The tension between our most precise "$L_{w\geq 1}$ + SR" fit and the data is $3.9\sigma$, with a $p$-value of $11.5 \times 10^{-5}$, to be compared with $8.3 \times 10^{-5}$ quoted by HFAG [9]. The precision of this prediction is limited by that of the input measurements and LQCD inputs, and can be systematically improved with new data from Belle II or LHCb.

To derive a SM prediction for $R(D^*)$, the authors of Ref. [34] used the measured $R_2(1)$ form factor ratio [9] and the QCDSR predictions to obtain $R_0(1) = 1.14 \pm 0.11$. In comparison, our "$L_{w\geq 1}$ + SR" fit results yield

$$R_0(1) = 1.17 \pm 0.02, \qquad R_3(1) = 1.19 \pm 0.03. \quad (41)$$

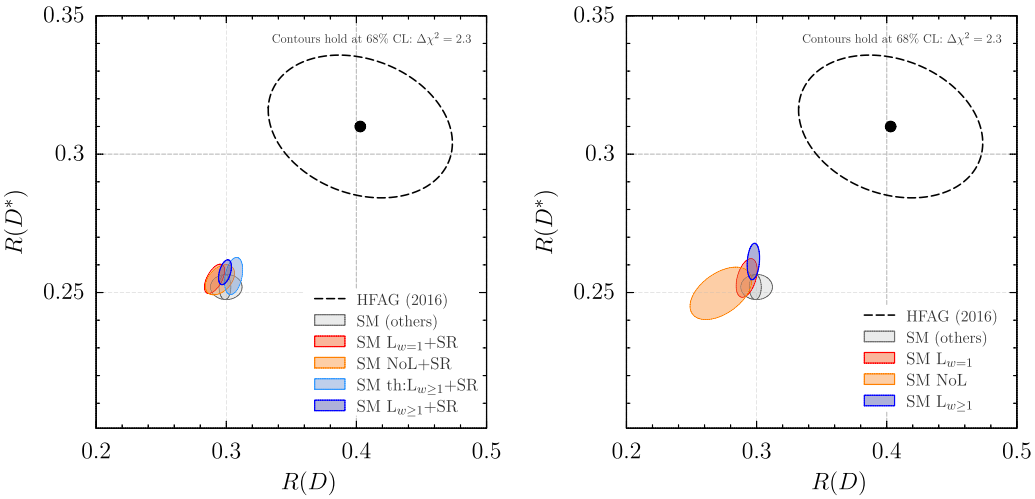


FIG. 4. The SM predictions for $R(D)$ and $R(D^*)$, imposing (left) or not imposing (right) the QCDSR constraints (see Table IV). Gray ellipses show other SM predictions (last three rows of Table IV). The black ellipse shows the world average of the data [9]. The contours are 68% C.L. ($\Delta\chi^2 = 2.3$), hence the nearly $4\sigma$ tension.

TABLE IV. The $R(D)$ and $R(D^*)$ predictions for our fit scenarios, the world average of the data, and other theory predictions. The fit scenarios are described in the text and in Table I. The bold numbers are our most precise predictions.

| Scenario | $R(D)$ | $R(D^*)$ | Correlation |
|---|---|---|---|
| $L_{w=1}$ | $0.292 \pm 0.005$ | $0.255 \pm 0.005$ | 41% |
| $L_{w=1}$ + SR | $0.291 \pm 0.005$ | $0.255 \pm 0.003$ | 57% |
| NoL | $0.273 \pm 0.016$ | $0.250 \pm 0.006$ | 49% |
| NoL + SR | $0.295 \pm 0.007$ | $0.255 \pm 0.004$ | 43% |
| $L_{w\geq 1}$ | $0.298 \pm 0.003$ | $0.261 \pm 0.004$ | 19% |
| $L_{w\geq 1}$ + SR | $\mathbf{0.299 \pm 0.003}$ | $\mathbf{0.257 \pm 0.003}$ | **44%** |
| th:$L_{w\geq 1}$ + SR | $0.306 \pm 0.005$ | $0.256 \pm 0.004$ | 33% |
| Data [9] | $0.403 \pm 0.047$ | $0.310 \pm 0.017$ | −23% |
| Refs. [53,57,59] | $0.300 \pm 0.008$ | ... | ... |
| Ref. [58] | $0.299 \pm 0.003$ | ... | ... |
| Ref. [34] | ... | $0.252 \pm 0.003$ | ... |

The precision on $R_0(1)$ improves five-fold compared to Ref. [34] and is in good agreement.

In Fig. 5 we illustrate the impacts NP might have on the allowed $R(D) - R(D^*)$ regions, assuming the dominance of one new physics operator in a standard four-Fermi basis. NP couplings are permitted to have an arbitrary phase, generating allowed regions rather than single contours. We display the allowed regions generated for the "NoL + SR" best-fit values, the "$L_{w\geq 1}$ + SR" best-fit values, and for leading-order contributions only, i.e., $\alpha_s$, $\varepsilon_{c,b} \to 0$, with $\bar{\rho}_*^2 = 1.24$. The small variation between the "NoL + SR" and "$L_{w\geq 1}$ + SR" regions illustrates the good consistency of the predictions obtained with and without LQCD. In each plot, we also include for comparison the corresponding contours (dashed lines) produced by a NP $O_V - O_A$ coupling. The latter rescales $R(D)$ and $R(D^*)$ keeping their ratio fixed. Solid dots indicate the SM point for each case. For scalar currents, if NP only contributes to $O_S$ ($O_P$) then only $R(D)$ [$R(D^*)$] is affected in accordance with Eq. (10b) [Eq. (11a)], respectively. We plot the allowed regions for the $O_S \pm O_P$ linear combinations, which are also motivated by specific NP models.

## IV. SUMMARY AND OUTLOOK

We performed a novel combined fit of the $\overline{B} \to D l \bar{\nu}$ and $\overline{B} \to D^* l \bar{\nu}$ differential rates and angular distributions, consistently including the HQET relations to $\mathcal{O}(\Lambda_{\rm QCD}/m_{c,b}, \alpha_s)$. Under various fit scenarios, that use

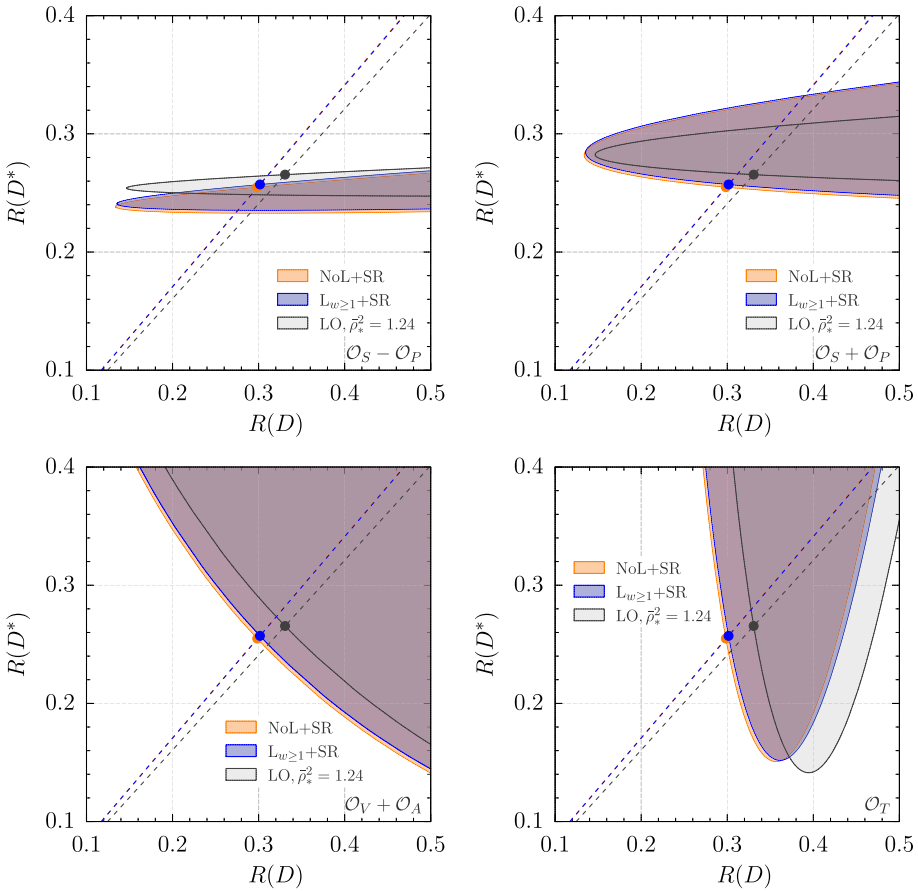


FIG. 5. The allowed ranges of $R(D) - R(D^*)$, due to one of the new physics operators in addition to the SM: $O_S - O_P$ (top left), $O_S + O_P$ (top right), $O_V + O_A$ (bottom left), and $O_T$ (bottom right).

or omit lattice QCD and QCD sum rule predictions, we constrained the leading and subleading Isgur-Wise functions. We thus obtained strong constraints on all form factors, and predictions for the form factor ratios $R_{1,2}$ as well as $R(D^{(*)})$, both in the SM and in arbitrary NP scenarios, valid at $\mathcal{O}(\alpha_s)$ and $\mathcal{O}(\Lambda_{\rm QCD}/m_{c,b})$. Our most precise prediction for $R(D^{(*)})$, in the "$\mathrm{L}_{w\geq 1}$ + SR" fit, using the experimental data and all lattice QCD and QCDSR inputs is

$$R(D) = 0.299 \pm 0.003,$$
$$R(D^*) = 0.257 \pm 0.003, \tag{42}$$

with a correlation of 44%. The same fit also yields $|V_{cb}| = (39.3 \pm 1.0) \times 10^{-3}$, which is in good agreement with existing exclusive determinations. All possible $b \to c$ current form factors were derived at $\mathcal{O}(\Lambda_{\rm QCD}/m_{c,b})$ and $\mathcal{O}(\alpha_s)$, including those for a tensor current, previously unavailable in the literature at this order. A lattice QCD calculation of the subleading Isgur-Wise functions, or even just those which arise from the chromomagnetic term in the subleading HQET Lagrangian ($\chi_{2,3}$), would be important to reduce hadronic uncertainties in both SM and NP predictions, complementary to a long-awaited lattice calculation of $R(D^*)$.

At the current level of experimental precision, our predictions agree up to mild tensions with previous results, which neglected the HQET relations for the uncertainties of the $\mathcal{O}(\Lambda_{\rm QCD}/m_{c,b})$ terms. Our fit results are consistent with one another, and at the current level of precision we find no inconsistencies between the data, lattice QCD results, and QCD sum rule predictions. Our fit using all available lattice QCD and QCD sum rule inputs and HQET to order $\mathcal{O}(\alpha_s, \Lambda_{\rm QCD}/m_{c,b})$ yields the most precise combined prediction for $R(D)$ and $R(D^*)$ to date. However, in principle, our fit need not require either lattice or sum rule input, and its precision can be improved simply as the statistics of future data increases.

The (moderate) tension between the measurements of $|V_{cb}|$ from inclusive and exclusive semileptonic decays probably cannot be resolved with current data. Understanding how the inclusive rate is made up from a sum of exclusive channels has been unclear from the data for a long time [60], and puzzles remain even in light of *BABAR* and Belle measurements [61,62]. A more detailed examination of the effects of the unitarity constraints and the precision extraction of $|V_{cb}|$ is the subject of ongoing work [55]. We are also implementing the full angular distributions of the measurable particles [63,64] into a software package, HAMMER [65,66], based on the state-of-the-art HQET predictions for all six $B \to D, D^*, D^{**}$ decay modes.

## ACKNOWLEDGMENTS

We thank Marat Freytsis, Ben Grinstein and Aneesh Manohar for helpful conversations. F. B. was supported by the Deutsche Forschungsgemeinschaft (DFG) Emmy-Noether Grant No. BE 6075/1-1. F. B. thanks Kim Scott and Robert Michaud for the kind hospitality in Houston where part of this work was carried out and inspiring conversations over good wine and food. Z. L. and M. P. were supported in part by the U.S. Department of Energy under contract DE-AC02-05CH11231. D. R. acknowledges support from the University of Cincinnati.

## APPENDIX A: THE $\mathcal{O}(\alpha_s)$ CORRECTIONS

In this appendix we summarize the explicit expressions for the $C_\Gamma(w)$ functions defined in Eq. (9), calculated in Ref. [27]. The following results use the $\overline{\rm MS}$ scheme and correspond to matching from QCD onto HQET at $\mu = \sqrt{m_c m_b}$:

$$C_S = \frac{1}{z(w-w_z)}[2z(w-w_z)\Omega(w) - ((w-1)(z+1)^2 r(w) - (z^2-1)\ln z)], \tag{A1a}$$

$$C_P = \frac{1}{2z^2(w-w_z)^2}[(z-1)[(w(z^3-(3+2w)z^2+z-1) + (z^2+3)z)r(w) + (z^2-1)\ln z] - 2z(w_z-w)(z-1+(z+1)z\ln z) + 4z^2(w-w_z)^2\Omega(w)], \tag{A1b}$$

$$C_{V_1} = \frac{1}{6z(w-w_z)}[2(w+1)((3w-1)z-z^2-1)r(w) + (12z(w_z-w) - (z^2-1)\ln z) + 4z(w-w_z)\Omega(w)], \tag{A1c}$$

$$C_{V_2} = \frac{-1}{6z^2(w-w_z)^2}[((4w^2+2w)z^2 - (2w^2+5w-1)z - (w+1)z^3+2)r(w) + z(2(z-1)(w_z-w) + (z^2-(4w-2)z+(3-2w))\ln z)], \tag{A1d}$$

$$C_{V_3} = \frac{1}{6z(w-w_z)^2}[((2w^2+5w-1)z^2 - (4w^2+2w)z - 2z^3+w+1)r(w) + (2z(z-1)(w_z-w) + ((3-2w)z^2+(2-4w)z+1)\ln z)], \tag{A1e}$$

$$C_{A_1} = \frac{1}{6z(w-w_z)}[2(w-1)((3w+1)z-z^2-1)r(w) + (12z(w_z-w) - (z^2-1)\ln z) + 4z(w-w_z)\Omega(w)], \tag{A1f}$$

$$C_{A_2} = \frac{-1}{6z^2(w-w_z)^2}[((4w^2-2w)z^2 + (2w^2-5w-1)z + (1-w)z^3+2)r(w) + z(2(z+1)(w_z-w) + (z^2-(4w+2)z+(2w+3))\ln z)], \tag{A1g}$$

$$C_{A_3} = \frac{1}{6z(w-w_z)^2}[(2z^3+(2w^2-5w-1)z^2 + (4w^2-2w)z - w + 1)r(w) + (2z(z+1)(w_z-w) - ((2w+3)z^2-(4w+2)z+1)\ln z)], \quad \text{(A1h)}$$

$$C_{T_1} = \frac{1}{3z(w-w_z)}[(w-1)((4w+2)z-z^2-1)r(w) + (6z(w_z-w)-(z^2-1)\ln z) + 2z(w-w_z)\Omega(w)], \quad \text{(A1i)}$$

$$C_{T_2} = \frac{2}{3z(w-w_z)}[(1-wz)r(w)+z\ln z], \quad \text{(A1j)}$$

$$C_{T_3} = \frac{2}{3(w-w_z)}[(w-z)r(w)+\ln z], \quad \text{(A1k)}$$

and $C_{T_4} = 0$. Here $z = m_c/m_b$, and the functions

$$\Omega(w) \equiv \frac{w}{2\sqrt{w^2-1}}[2\mathrm{Li}_2(1-w_-z) - 2\mathrm{Li}_2(1-w_+z) + \mathrm{Li}_2(1-w_+^2) - \mathrm{Li}_2(1-w_-^2)] - wr(w)\ln z + 1, \quad \text{(A2)}$$

where $\mathrm{Li}_2(x) = \int_x^0 \ln(1-t)/t\,dt$ is the dilogarithm, and

$$r(w) \equiv \frac{\ln w_+}{\sqrt{w^2-1}}, \qquad w_\pm \equiv w \pm \sqrt{w^2-1}, \qquad w_z \equiv \frac{1}{2}(z+1/z). \quad \text{(A3)}$$

At the zero recoil point, $w = 1$,

$$C_S(1) = -\frac{2}{3}, \qquad C_P(1) = \frac{2}{3},$$
$$C_{V_1}(1) = -\frac{4}{3} - \frac{1+z}{1-z}\ln z, \qquad C_{V_2}(1) = -\frac{2(1-z+z\ln z)}{3(1-z)^2},$$
$$C_{V_3}(1) = \frac{2z(1-z+\ln z)}{3(1-z)^2},$$
$$C_{A_1}(1) = -\frac{8}{3} - \frac{1+z}{1-z}\ln z,$$
$$C_{A_2}(1) = -\frac{2[3-2z-z^2+(5-z)z\ln z]}{3(1-z)^3},$$
$$C_{A_3}(1) = \frac{2z[1+2z-3z^2+(5z-1)\ln z]}{3(1-z)^3},$$
$$C_{T_1}(1) = -\frac{8}{3} - \frac{4(1+z)}{3(1-z)}\ln z, \qquad C_{T_2}(1) = 2C_{V_2}(1),$$
$$C_{T_3}(1) = -2C_{V_3}(1). \quad \text{(A4)}$$

Finally, for arbitrary matching scale $\mu$, one should add to Eq. (A1) the terms

$$C_{S,P}^{(\mu^2)} = C_{S,P}^{(m_b m_c)} - \frac{1}{3}[2wr(w)+1]\ln(m_c m_b/\mu^2), \quad \text{(A5a)}$$

$$C_{V_1,A_1}^{(\mu^2)} = C_{V_1,A_1}^{(m_b m_c)} - \frac{2}{3}[wr(w)-1]\ln(m_c m_b/\mu^2), \quad \text{(A5b)}$$

$$C_{T_1}^{(\mu^2)} = C_{T_1}^{(m_b m_c)} - \frac{1}{3}[2wr(w)-3]\ln(m_c m_b/\mu^2), \quad \text{(A5c)}$$

and all other $C_{\Gamma_j}^{(\mu^2)} = C_{\Gamma_j}^{(m_b m_c)}$, for $j \geq 2$.

## APPENDIX B: DULL CORRELATIONS

The correlation matrices for the fit scenarios are given in Tables V–XI.

TABLE V. The correlations of the "$L_{w=1}$" fit scenario.

| | $\lvert V_{cb}\rvert$ | $\mathcal{G}(1)$ | $\mathcal{F}(1)$ | $\bar{\rho}_*^2$ | $\hat{\chi}_2(1)$ | $\hat{\chi}_2'(1)$ | $\hat{\chi}_3'(1)$ | $\eta(1)$ | $m_b^{1S}$ | $\delta m_{bc}$ |
|---|---|---|---|---|---|---|---|---|---|---|
| $\lvert V_{cb}\rvert$ | 1.00 | −0.16 | −0.18 | 0.30 | −0.13 | 0.28 | 0.11 | 0.04 | −0.01 | 0.00 |
| $\mathcal{G}(1)$ | −0.16 | 1.00 | 0.06 | −0.11 | 0.03 | −0.04 | −0.09 | −0.23 | 0.00 | −0.00 |
| $\mathcal{F}(1)$ | −0.18 | 0.06 | 1.00 | 0.18 | −0.00 | 0.08 | 0.21 | −0.02 | 0.01 | −0.00 |
| $\bar{\rho}_*^2$ | 0.30 | −0.11 | 0.18 | 1.00 | 0.67 | −0.47 | 0.82 | 0.13 | −0.16 | 0.01 |
| $\hat{\chi}_2(1)$ | −0.13 | 0.03 | −0.00 | 0.67 | 1.00 | −0.87 | 0.82 | −0.11 | 0.07 | −0.01 |
| $\hat{\chi}_2'(1)$ | 0.28 | −0.04 | 0.08 | −0.47 | −0.87 | 1.00 | −0.47 | 0.01 | 0.01 | −0.00 |
| $\hat{\chi}_3'(1)$ | 0.11 | −0.09 | 0.21 | 0.82 | 0.82 | −0.47 | 1.00 | −0.12 | 0.12 | −0.02 |
| $\eta(1)$ | 0.04 | −0.23 | −0.02 | 0.13 | −0.11 | 0.01 | −0.12 | 1.00 | −0.52 | 0.05 |
| $m_b^{1S}$ | −0.01 | 0.00 | 0.01 | −0.16 | 0.07 | 0.01 | 0.12 | −0.52 | 1.00 | 0.00 |
| $\delta m_{bc}$ | 0.00 | −0.00 | −0.00 | 0.01 | −0.01 | −0.00 | −0.02 | 0.05 | 0.00 | 1.00 |

TABLE VI. The correlations of the "$L_{w=1}$ + SR" fit scenario.

| | $\lvert V_{cb}\rvert$ | $\mathcal{G}(1)$ | $\mathcal{F}(1)$ | $\bar{\rho}_*^2$ | $\hat{\chi}_2(1)$ | $\hat{\chi}_2'(1)$ | $\hat{\chi}_3'(1)$ | $\eta(1)$ | $\eta'(1)$ | $m_b^{1S}$ | $\delta m_{bc}$ |
|---|---|---|---|---|---|---|---|---|---|---|---|
| $\lvert V_{cb}\rvert$ | 1.00 | −0.12 | −0.32 | 0.48 | −0.02 | 0.02 | 0.14 | 0.05 | 0.02 | −0.02 | 0.00 |
| $\mathcal{G}(1)$ | −0.12 | 1.00 | 0.14 | −0.05 | 0.04 | 0.01 | −0.14 | −0.23 | 0.09 | −0.00 | −0.00 |
| $\mathcal{F}(1)$ | −0.32 | 0.14 | 1.00 | 0.04 | −0.07 | −0.01 | 0.24 | −0.02 | −0.11 | −0.03 | 0.01 |
| $\bar{\rho}_*^2$ | 0.48 | −0.05 | 0.04 | 1.00 | −0.09 | −0.04 | 0.57 | 0.32 | 0.08 | −0.45 | 0.04 |
| $\hat{\chi}_2(1)$ | −0.02 | 0.04 | −0.07 | −0.09 | 1.00 | −0.03 | 0.17 | −0.06 | −0.20 | 0.04 | −0.00 |
| $\hat{\chi}_2'(1)$ | 0.02 | 0.01 | −0.01 | −0.04 | −0.03 | 1.00 | 0.06 | −0.02 | −0.09 | 0.01 | −0.00 |
| $\hat{\chi}_3'(1)$ | 0.14 | −0.14 | 0.24 | 0.57 | 0.17 | 0.06 | 1.00 | 0.08 | 0.38 | −0.03 | 0.00 |
| $\eta(1)$ | 0.05 | −0.23 | −0.02 | 0.32 | −0.06 | −0.02 | 0.08 | 1.00 | −0.14 | −0.48 | 0.05 |
| $\eta'(1)$ | 0.02 | 0.09 | −0.11 | 0.08 | −0.20 | −0.09 | 0.38 | −0.14 | 1.00 | 0.08 | −0.01 |
| $m_b^{1S}$ | −0.02 | −0.00 | −0.03 | −0.45 | 0.04 | 0.01 | −0.03 | −0.48 | 0.08 | 1.00 | 0.01 |
| $\delta m_{bc}$ | 0.00 | −0.00 | 0.01 | 0.04 | −0.00 | −0.00 | 0.00 | 0.05 | −0.01 | 0.01 | 1.00 |

TABLE VII. The correlations of the "NoL" fit scenario.

| | $\bar{\rho}_*^2$ | $\hat{\chi}_2(1)$ | $\hat{\chi}_2'(1)$ | $\hat{\chi}_3'(1)$ | $\eta(1)$ | $m_b^{1S}$ | $\delta m_{bc}$ |
|---|---|---|---|---|---|---|---|
| $\bar{\rho}_*^2$ | 1.00 | −0.22 | −0.18 | −0.03 | 0.46 | −0.22 | 0.01 |
| $\hat{\chi}_2(1)$ | −0.22 | 1.00 | −0.41 | 0.94 | −0.92 | 0.33 | −0.03 |
| $\hat{\chi}_2'(1)$ | −0.18 | −0.41 | 1.00 | −0.19 | 0.08 | −0.02 | −0.00 |
| $\hat{\chi}_3'(1)$ | −0.03 | 0.94 | −0.19 | 1.00 | −0.88 | 0.32 | −0.03 |
| $\eta(1)$ | 0.46 | −0.92 | 0.08 | −0.88 | 1.00 | −0.35 | 0.02 |
| $m_b^{1S}$ | −0.22 | 0.33 | −0.02 | 0.32 | −0.35 | 1.00 | 0.00 |
| $\delta m_{bc}$ | 0.01 | −0.03 | −0.00 | −0.03 | 0.02 | 0.00 | 1.00 |

TABLE VIII. The correlations of the "NoL + SR" fit scenario.

| | $\bar{\rho}_*^2$ | $\hat{\chi}_2(1)$ | $\hat{\chi}_2'(1)$ | $\hat{\chi}_3'(1)$ | $\eta(1)$ | $\eta'(1)$ | $m_b^{1S}$ | $\delta m_{bc}$ |
|---|---|---|---|---|---|---|---|---|
| $\bar{\rho}_*^2$ | 1.00 | −0.15 | −0.07 | 0.57 | 0.44 | −0.11 | −0.31 | 0.03 |
| $\hat{\chi}_2(1)$ | −0.15 | 1.00 | −0.02 | 0.07 | −0.15 | −0.09 | 0.02 | −0.00 |
| $\hat{\chi}_2'(1)$ | −0.07 | −0.02 | 1.00 | 0.03 | −0.07 | −0.05 | 0.00 | −0.00 |
| $\hat{\chi}_3'(1)$ | 0.57 | 0.07 | 0.03 | 1.00 | 0.17 | 0.16 | 0.00 | −0.00 |
| $\eta(1)$ | 0.44 | −0.15 | −0.07 | 0.17 | 1.00 | −0.40 | 0.09 | −0.01 |
| $\eta'(1)$ | −0.11 | −0.09 | −0.05 | 0.16 | −0.40 | 1.00 | 0.02 | −0.00 |
| $m_b^{1S}$ | −0.31 | 0.02 | 0.00 | 0.00 | 0.09 | 0.02 | 1.00 | 0.01 |
| $\delta m_{bc}$ | 0.03 | −0.00 | −0.00 | −0.00 | −0.01 | −0.00 | 0.01 | 1.00 |

TABLE IX. The correlations of the "$L_{w\geq 1}$" fit scenario.

| | $\lvert V_{cb}\rvert \times 10^3$ | $\mathcal{G}(1)$ | $\mathcal{F}(1)$ | $\bar{\rho}_*^2$ | $\chi_2(1)$ | $\chi_2'$ | $\chi_3'$ | $\eta(1)$ | $m_b^{1S}$ | $\delta m_{bc}$ |
|---|---|---|---|---|---|---|---|---|---|---|
| $\lvert V_{cb}\rvert \times 10^3$ | 1.00 | −0.30 | −0.16 | 0.18 | −0.13 | 0.28 | 0.07 | 0.01 | 0.00 | 0.00 |
| $\mathcal{G}(1)$ | −0.30 | 1.00 | 0.08 | −0.28 | −0.04 | −0.04 | −0.16 | −0.23 | 0.01 | −0.00 |
| $\mathcal{F}(1)$ | −0.16 | 0.08 | 1.00 | 0.38 | 0.18 | −0.10 | 0.32 | 0.00 | 0.01 | −0.00 |
| $\bar{\rho}_*^2$ | 0.18 | −0.28 | 0.38 | 1.00 | 0.64 | −0.44 | 0.80 | 0.18 | −0.22 | 0.01 |
| $\hat{\chi}_2(1)$ | −0.13 | −0.04 | 0.18 | 0.64 | 1.00 | −0.79 | 0.89 | −0.17 | 0.21 | −0.03 |
| $\hat{\chi}_2'(1)$ | 0.28 | −0.04 | −0.10 | −0.44 | −0.79 | 1.00 | −0.48 | 0.05 | −0.13 | 0.02 |
| $\hat{\chi}_3'(1)$ | 0.07 | −0.16 | 0.32 | 0.80 | 0.89 | −0.48 | 1.00 | −0.12 | 0.18 | −0.03 |
| $\eta(1)$ | 0.01 | −0.23 | 0.00 | 0.18 | −0.17 | 0.05 | −0.12 | 1.00 | −0.54 | 0.05 |
| $m_b^{1S}$ | 0.00 | 0.01 | 0.01 | −0.22 | 0.21 | −0.13 | 0.18 | −0.54 | 1.00 | 0.01 |
| $\delta m_{bc}$ | 0.00 | −0.00 | −0.00 | 0.01 | −0.03 | 0.02 | −0.03 | 0.05 | 0.01 | 1.00 |

TABLE X. The correlations of the "$L_{w\geq 1}$ + SR" fit scenario.

| | $\lvert V_{cb}\rvert$ | $\mathcal{G}(1)$ | $\mathcal{F}(1)$ | $\bar{\rho}_*^2$ | $\hat{\chi}_2(1)$ | $\hat{\chi}_2'(1)$ | $\hat{\chi}_3'(1)$ | $\eta(1)$ | $\eta'(1)$ | $m_b^{1S}$ | $\delta m_{bc}$ |
|---|---|---|---|---|---|---|---|---|---|---|---|
| $\lvert V_{cb}\rvert$ | 1.00 | −0.27 | −0.28 | 0.33 | −0.05 | 0.00 | 0.21 | 0.03 | 0.13 | −0.01 | 0.00 |
| $\mathcal{G}(1)$ | −0.27 | 1.00 | 0.24 | −0.26 | 0.07 | 0.02 | −0.22 | −0.22 | −0.27 | −0.02 | 0.00 |
| $\mathcal{F}(1)$ | −0.28 | 0.24 | 1.00 | 0.15 | −0.06 | −0.02 | 0.25 | −0.03 | −0.19 | −0.01 | 0.00 |
| $\bar{\rho}_*^2$ | 0.33 | −0.26 | 0.15 | 1.00 | −0.13 | −0.08 | 0.72 | 0.35 | 0.13 | −0.49 | 0.05 |
| $\hat{\chi}_2(1)$ | −0.05 | 0.07 | −0.06 | −0.13 | 1.00 | −0.04 | 0.25 | −0.10 | −0.11 | 0.06 | −0.01 |
| $\hat{\chi}_2'(1)$ | 0.00 | 0.02 | −0.02 | −0.08 | −0.04 | 1.00 | 0.07 | −0.05 | −0.06 | 0.04 | −0.00 |
| $\hat{\chi}_3'(1)$ | 0.21 | −0.22 | 0.25 | 0.72 | 0.25 | 0.07 | 1.00 | 0.16 | 0.19 | −0.06 | 0.01 |
| $\eta(1)$ | 0.03 | −0.22 | −0.03 | 0.35 | −0.10 | −0.05 | 0.16 | 1.00 | 0.05 | −0.48 | 0.05 |
| $\eta'(1)$ | 0.13 | −0.27 | −0.19 | 0.13 | −0.11 | −0.06 | 0.19 | 0.05 | 1.00 | 0.04 | 0.00 |
| $m_b^{1S}$ | −0.01 | −0.02 | −0.01 | −0.49 | 0.06 | 0.04 | −0.06 | −0.48 | 0.04 | 1.00 | 0.01 |
| $\delta m_{bc}$ | 0.00 | 0.00 | 0.00 | 0.05 | −0.01 | −0.00 | 0.01 | 0.05 | 0.00 | 0.01 | 1.00 |

TABLE XI. The correlations of the "th: $L_{w\geq 1}$ + SR" fit scenario.

| | $\mathcal{G}(1)$ | $\mathcal{F}(1)$ | $\bar{\rho}_*^2$ | $\hat{\chi}_2(1)$ | $\hat{\chi}_2'(1)$ | $\hat{\chi}_3'(1)\eta(1)$ | $\eta(1)$ | $\eta'(1)$ | $m_b^{1S}$ | $\delta m_{bc}$ |
|---|---|---|---|---|---|---|---|---|---|---|
| $\mathcal{G}(1)$ | 1.00 | 0.00 | −0.15 | 0.01 | −0.00 | −0.02 | −0.25 | −0.40 | 0.01 | −0.00 |
| $\mathcal{F}(1)$ | 0.00 | 1.00 | −0.00 | −0.00 | −0.00 | −0.00 | −0.00 | −0.00 | −0.00 | −0.00 |
| $\bar{\rho}_*^2$ | −0.15 | −0.00 | 1.00 | −0.27 | −0.13 | 0.81 | 0.08 | −0.07 | −0.24 | 0.02 |
| $\hat{\chi}_2(1)$ | 0.01 | −0.00 | −0.27 | 1.00 | 0.00 | 0.01 | 0.01 | 0.03 | −0.01 | 0.00 |
| $\hat{\chi}_2'(1)$ | −0.00 | −0.00 | −0.13 | 0.00 | 1.00 | −0.01 | −0.01 | 0.01 | 0.01 | −0.00 |
| $\hat{\chi}_3'(1)$ | −0.02 | −0.00 | 0.81 | 0.01 | −0.01 | 1.00 | −0.02 | −0.09 | 0.04 | −0.00 |
| $\eta(1)$ | −0.25 | −0.00 | 0.08 | 0.01 | −0.01 | −0.02 | 1.00 | 0.11 | −0.48 | 0.04 |
| $\eta'(1)$ | −0.40 | −0.00 | −0.07 | 0.03 | 0.01 | −0.09 | 0.11 | 1.00 | 0.07 | −0.01 |
| $m_b^{1S}$ | 0.01 | −0.00 | −0.24 | −0.01 | 0.01 | 0.04 | −0.48 | 0.07 | 1.00 | 0.00 |
| $\delta m_{bc}$ | −0.00 | −0.00 | 0.02 | 0.00 | −0.00 | −0.00 | 0.04 | −0.01 | 0.00 | 1.00 |


[1] N. Isgur and M. B. Wise, Phys. Lett. B **232**, 113 (1989).
[2] N. Isgur and M. B. Wise, Phys. Lett. B **237**, 527 (1990).
[3] J. P. Lees *et al.* (*BABAR* Collaboration), Phys. Rev. Lett. **109**, 101802 (2012).
[4] J. P. Lees *et al.* (*BABAR* Collaboration), Phys. Rev. D **88**, 072012 (2013).
[5] M. Huschle *et al.* (Belle Collaboration), Phys. Rev. D **92**, 072014 (2015).
[6] A. Abdesselam *et al.* (Belle Collaboration), arXiv: 1603.06711.
[7] A. Abdesselam *et al.* (Belle Collaboration), arXiv: 1608.06391.
[8] R. Aaij *et al.* (LHCb Collaboration), Phys. Rev. Lett. **115**, 111803 (2015); **115**, 159901(E) (2015).
[9] Y. Amhis *et al.* (Heavy Flavor Averaging Group Collaboration), arXiv:1612.07233, and updates at http://www.slac.stanford.edu/xorg/hfag/.
[10] M. Freytsis, Z. Ligeti, and J. T. Ruderman, Phys. Rev. D **92**, 054018 (2015).
[11] J. Charles, S. Descotes-Genon, Z. Ligeti, S. Monteil, M. Papucci, and K. Trabelsi, Phys. Rev. D **89**, 033016 (2014).
[12] F. U. Bernlochner and Z. Ligeti, Phys. Rev. D **95**, 014022 (2017).
[13] M. E. Luke, Phys. Lett. B **252**, 447 (1990).
[14] M. Neubert and V. Rieckert, Nucl. Phys. **B382**, 97 (1992).
[15] A. V. Manohar and M. B. Wise, *Heavy Quark Physics* (Cambridge University Press, Cambridge, England, 2000).
[16] M. Neubert, Phys. Rep. **245**, 259 (1994).
[17] A. F. Falk, H. Georgi, B. Grinstein, and M. B. Wise, Nucl. Phys. **B343**, 1 (1990).
[18] J. D. Bjorken, in *Gauge Bosons and Heavy Quarks: Proceedings, 18th SLAC Summer Institute on Particle Physics (SSI 90), July 16–27, 1990*, edited by J. F. Hawthorne (SLAC, Stanford, 1991), p. 167.
[19] A. F. Falk, Nucl. Phys. **B378**, 79 (1992).
[20] A. F. Falk and M. Neubert, Phys. Rev. D **47**, 2965 (1993).
[21] M. E. Luke and A. V. Manohar, Phys. Lett. B **286**, 348 (1992).
[22] B. Grinstein and Z. Ligeti, Phys. Lett. B **526**, 345 (2002); **601**, 236(E) (2004).
[23] M. Neubert, Z. Ligeti, and Y. Nir, Phys. Lett. B **301**, 101 (1993).
[24] M. Neubert, Z. Ligeti, and Y. Nir, Phys. Rev. D **47**, 5060 (1993).
[25] Z. Ligeti, Y. Nir, and M. Neubert, Phys. Rev. D **49**, 1302 (1994).

[26] A. F. Falk and B. Grinstein, Phys. Lett. B **249**, 314 (1990).
[27] M. Neubert, Nucl. Phys. **B371**, 149 (1992).
[28] M. Tanaka and R. Watanabe, Phys. Rev. D **87**, 034028 (2013).
[29] C. Patrignani *et al.* (Particle Data Group Collaboration), Chin. Phys. C **40**, 100001 (2016).
[30] M. A. Shifman and M. B. Voloshin, Yad. Fiz. **47**, 801 (1988) [Sov. J. Nucl. Phys. **47**, 511 (1988)].
[31] C. G. Boyd, B. Grinstein, and A. V. Manohar, Phys. Rev. D **54**, 2081 (1996).
[32] A. V. Manohar, Lect. Notes Phys. **479**, 311 (1997).
[33] A. Sirlin, Nucl. Phys. **B196**, 83 (1982).
[34] S. Fajfer, J. F. Kamenik, and I. Nisandzic, Phys. Rev. D **85**, 094025 (2012).
[35] M. Neubert and C. T. Sachrajda, Nucl. Phys. **B438**, 235 (1995).
[36] M. E. Luke, A. V. Manohar, and M. J. Savage, Phys. Rev. D **51**, 4924 (1995).
[37] M. Beneke and V. M. Braun, Nucl. Phys. **B426**, 301 (1994).
[38] I. I. Y. Bigi, M. A. Shifman, N. G. Uraltsev, and A. I. Vainshtein, Phys. Rev. D **50**, 2234 (1994).
[39] M. Beneke, V. M. Braun, and V. I. Zakharov, Phys. Rev. Lett. **73**, 3058 (1994).
[40] A. H. Hoang, Z. Ligeti, and A. V. Manohar, Phys. Rev. Lett. **82**, 277 (1999).
[41] A. H. Hoang, Z. Ligeti, and A. V. Manohar, Phys. Rev. D **59**, 074017 (1999).
[42] A. H. Hoang, Phys. Rev. D **61**, 034005 (1999).
[43] M. Beneke, Phys. Lett. B **434**, 115 (1998).
[44] A. Czarnecki, K. Melnikov, and N. Uraltsev, Phys. Rev. Lett. **80**, 3189 (1998).
[45] Z. Ligeti and F. J. Tackmann, Phys. Rev. D **90**, 034021 (2014).
[46] C. G. Boyd, B. Grinstein, and R. F. Lebed, Nucl. Phys. **B461**, 493 (1996).
[47] C. G. Boyd, B. Grinstein, and R. F. Lebed, Phys. Rev. D **56**, 6895 (1997).
[48] I. Caprini, L. Lellouch, and M. Neubert, Nucl. Phys. **B530**, 153 (1998).
[49] C. G. Boyd and M. J. Savage, Phys. Rev. D **56**, 303 (1997).
[50] R. J. Hill, *Proceedings, 4th Conference on Flavor Physics and CP Violation (FPCP 2006): Vancouver, British Columbia, Canada, April 9–12, 2006*, eConf C060409, 027 (2006).
[51] C. Bourrely, I. Caprini, and L. Lellouch, Phys. Rev. D **79**, 013008 (2009); **82**, 099902(E) (2010).
[52] J. A. Bailey *et al.* (Fermilab Lattice and MILC Collaborations), Phys. Rev. D **89**, 114504 (2014).
[53] J. A. Bailey *et al.* (Fermilab Lattice and MILC Collaborations), Phys. Rev. D **92**, 034506 (2015).
[54] A. Abdesselam *et al.* (Belle Collaboration), arXiv:1702.01521.
[55] F. Bernlochner, Z. Ligeti, M. Papucci, and D. J. Robinson (to be published).
[56] R. Glattauer *et al.* (Belle Collaboration), Phys. Rev. D **93**, 032006 (2016).
[57] S. Aoki *et al.* (Flavour Lattice Averaging Group Collaboration), Eur. Phys. J. C **77**, 112 (2017), and updates at http://itpwiki.unibe.ch/flag/.
[58] D. Bigi and P. Gambino, Phys. Rev. D **94**, 094008 (2016).
[59] H. Na, C. M. Bouchard, G. P. Lepage, C. Monahan, and J. Shigemitsu (HPQCD Collaboration), Phys. Rev. D **92**, 054510 (2015); **93**, 119906(E) (2016).
[60] J. D. Richman and P. R. Burchat, Rev. Mod. Phys. **67**, 893 (1995).
[61] F. U. Bernlochner, Z. Ligeti, and S. Turczyk, Phys. Rev. D **85**, 094033 (2012).
[62] F. U. Bernlochner, D. Biedermann, H. Lacker, and T. Luck, Eur. Phys. J. C **74**, 2914 (2014).
[63] Z. Ligeti, M. Papucci, and D. J. Robinson, J. High Energy Phys. 01 (2017) 083.
[64] R. Alonso, A. Kobach, and J. Martin Camalich, Phys. Rev. D **94**, 094021 (2016).
[65] S. Duell, F. Bernlochner, Z. Ligeti, M. Papucci, and D. Robinson, *Proc. Sci.*, ICHEP2016 (2016) 1074.
[66] F. Bernlochner, S. Duell, Z. Ligeti, M. Papucci, and D. J. Robinson (to be published).